

**Synthesis and Characterization of ZnO based  
Graphene Nanoplatelets Nanocomposites**



**Thesis**

**M.S Physics**

**By**

**Muhammad Saleem**

**Reg. No. 162-FBAS/MSPHY/S13**

**Supervised by**

**Dr. Javed Iqbal Saggu**

**Department of Physics**

**Faculty of Basic and Applied Sciences**

**International Islamic University Islamabad**

**(2015)**



Accession No TH15199

P. 8

MS

620.5

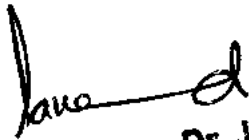
MUS

wood, nature materials

Technology

## Certificate

This is to certify that the work contained in this thesis entitled: **“Synthesis and Characterization of ZnO based Graphene Nanoplatelets Nanocomposites”** has been carried out by **Muhammad Saleem (162-FBAS/MSPHY/S13)** in Laboratory of Nanoscience and Technology (LNT) under my supervision. In my opinion, this is fully adequate in scope and quality for the degree of Master of Sciences (MS) in Physics.



**Dr. Javed Iqbal Saggu**  
Assistant Professor (Physics)  
International Islamic University  
Islamabad.

Supervisor

Dr. Javed Iqbal Saggu

Department of Physics

International Islamic University, Islamabad.

**Synthesis and Characterization of ZnO based  
Graphene Nanoplatelets Nanocomposites**

**By**

**Muhammad Saleem**

162-FBAS/MSPHY/S13

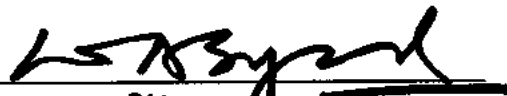
A thesis submitted to

**Department of Physics**

For the award of the degree of

**MS Physics**

Signature: \_\_\_\_\_

  
CHAIRMAN  
DEPT. OF PHYSICS  
International Islamic University  
Islamabad

6/11/15

(Chairman, Department of Physics, IIUI)

Signature: \_\_\_\_\_

(Dean FBAS, IIU, Islamabad)

## FINAL APPROVAL

It is certified that the work presented in this thesis entitled “**Synthesis and Characterization of ZnO based Graphene Nanoplatelets Nanocomposites**” by **Mr. Muhammad Saleem** bearing **Registration No. 162-FBAS/MSPHY/S13** is of sufficient standard in scope and quality for the award of degree of MS Physics from International Islamic University, Islamabad.

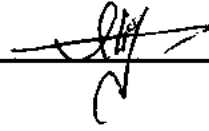
### COMMITTEE

#### **External Examiner**

Dr Muhammad Atif

Department of Physics

Air University, Islamabad



---

#### **Internal Examiner**

Dr. Naeem Ahmed

Department of Physics

FBAS, IIU Islamabad



---

#### **Supervisor**

Dr. Javed Iqbal Saggu

Department of Physics

FBAS, IIU Islamabad



---

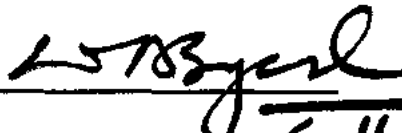
**Dr. Javed Iqbal Saggu:**  
Assistant Professor (Physics)  
International Islamic University  
Islamabad.

#### **Chairman**

Dr. Syed Waqar Adil Syed

Department of Physics

FBAS, IIU Islamabad



---

6.11.15

بِسْمِ اللَّهِ الرَّحْمَنِ الرَّحِيمِ

## Declaration

I hereby declare that this thesis work, neither as a whole nor a part of it has been copied out from any source. Further, work presented in this dissertation has not been submitted in support of any application for any other degree or qualification to any other university or institute and is considerable under the plagiarism rules of Higher Education Commission (HEC), Pakistan. Plagiarism report is generated by software turnitin through ID 594409043 with similarity index 7 %. it is also declare that if there is any issue regarding plagiarism, I myself will be responsible.

Signature: *M. Saleem*

Name: Muhammad Saleem

Reg.No.162-FBAS-MSPHY/S13

# **DEDICATION**

**To**

*My niece Faiza Rasheed (late)*

## ACKNOWLEDGEMENT

“In the name of Allah, the Most Gracious and the Most Merciful”

Alhamdulillah, all praises to Allah for the strengths and his blessings in completing this thesis. I offer my humblest and sincere words of thanks to his Holly Prophet Mohammad (P.B.U.H) who is forever a source of guidance and knowledge for humanity.

Special appreciation goes to my supervisor, **Dr Javed Iqbal Saggi**, for his supervision and constant support. His invaluable help of constructive comments and suggestions throughout the experimental and thesis works have contributed to the success of this research. Not forgotten, my appreciation to external examiner, Prof Dr.Muhammad Atif. He provided me constructive criticism which helped me develop a broader perspective to my thesis.

I would like to express my appreciation to my internal examiner, Dr.Muhammad Naeem. He generously gave their time to offer me valuable comments toward improving my work. My acknowledgement also goes to all the technicians and office staffs of International Islamic university for their co-operations.

Sincere thanks to all my friends especially, Umar Farooq, Muhammad Akhtar and others for their kindness and moral support during my study. Thanks for the friendship and memories.

Last but not least, my deepest gratitude goes to my beloved mother; for their endless love, prayers and encouragement. , I would like to thank my wife. She was always there cheering me up and stood by me through the good times and bad. To those who indirectly contributed in this research, your kindness means a lot to me.

Thank you very much.

Muhammad Saleem

## Table of Contents

<b>1</b>	<b>Chapter No. 1</b>	<b>Introduction.....</b>	<b>1</b>
	1.1	Composites .....	1
	1.1.1	Basis of composite materials.....	2
	1.1.1.1	Natural composite materials.....	2
	1.1.1.2	Man made composite materials.....	2
	1.1.2	Classification of composites on the basis of matrices.....	2
	1.1.2.1	Composite materials based on metal matrix.....	2
	1.1.2.2	Composites materials based on ceramic matrix .....	3
	1.1.2.3	Composites materials based on polymer matrix.....	3
	1.1.2.4	Composite materials based on graphene and chemically converted graphene...3	
	1.1.3	Classification of graphene-inorganic nanocomposites.....	5
	1.1.4	Classification of nanocomposites based on structure.....	5
	1.1.5	Applications of grapheme inorganic nanocomposites .....	6
	1.1.5.1	Catalysis.....	6
	1.1.5.2	Photo catalysis.....	7
	1.1.5.3	Energy storage and conversion.....	7
	1.1.5.4	Solar cells .....	7
	1.1.5.5	Fuel cells.....	8
	1.1.5.6	Gas detector .....	8
	1.2	History of Graphene .....	9
	1.2.1	Carbon Allotropes .....	9
	1.2.2	Graphene hybridization and bonding .....	10
	1.2.3	Crystal Structure.....	12

1.2.4	Brillouianzone .....	15
1.2.5	Graphite and Bi-layer graphene .....	15
1.2.6	Properties and application of graphene .....	16
1.2.7	Synthesismethods of graphene .....	17
1.2.8	Graphene nanoplatelets .....	17
1.2.9	Why use GNPs .....	18
1.2.10	Applications .....	18
1.3	Zinc Oxide (ZnO) .....	20
1.3.1	ZnO structure .....	20
1.3.2	Applications .....	22
<b>2</b>	<b>Chapter No.2 Analytical Techniques .....</b>	<b>23</b>
2.1	X-ray Diffraction (XRD) .....	23
2.1.1	Introduction .....	23
2.1.2	X-rays .....	24
2.1.3	Bragg's Law .....	25
2.2	Field Emission Electron Microscopy (FESEM) .....	26
2.2.1	FESEM working .....	26
2.2.2	Vacuum .....	26
2.2.3	Field Emission Source .....	26
2.2.4	Anode .....	26
2.2.5	Electromagnetic Lenses .....	27
2.2.6	Depth of Field .....	27
2.2.7	Electron beam and sample interaction .....	28
2.2.8	Applications .....	28

2.3	Energy-Dispersive Spectroscopy (EDS) .....	28
2.4	Fourier Transform Infra-red Spectroscopy (FTIR) .....	29
2.4.1	Procedure.....	31
2.5	Photoluminescence Spectroscopy (PL) .....	31
2.6	Raman Spectroscopy .....	32
2.7	Diffusion Reflectance Spectroscopy (DRS).....	34
<b>3</b>	<b>Chapter No.3            Synthesis Techniques.....</b>	<b>37</b>
3.1	Synthesis of graphene–inorganic nanocomposites .....	37
3.1.1	In situ synthesis method .....	37
3.1.1.1	Advantages .....	37
3.1.2	Ex situ synthesis method .....	37
3.1.2.1	Advantages .....	38
3.1.2.2	Covalent interactions .....	38
3.1.2.3	Non-covalent interactions.....	38
3.2	Constituent’s Materials.....	38
3.3	Preparation of ZnO nanostructures.....	38
3.4	Dispersibility of graphene nano platelet (GNP) .....	40
3.5	Uniform dispersion of graphene nano platelets (GNPs).....	41
3.5.1	Ultrasonication .....	41
3.6	Development of nanocomposites.....	41
3.7	Fabrication Process of GNPs-ZnO nanocomposites .....	42
1.1	Preparation of Agar diffusion assay for Antibacterial Test.....	43
<b>4</b>	<b>Chapter No.4            Results &amp; Discussions .....</b>	<b>44</b>
4.1	X-ray Diffraction Analysis:.....	44

4.2	Morphology of GNP-ZnO nanocomposites .....	47
4.3	EDX of GNPs and GNP-ZnO nanocomposites.....	50
4.4	Vibrational study of GNPs-ZnO nanocomposites.....	52
4.5	FTIR Analyses of GNP-ZnO nanocomposites .....	53
4.6	Optical properties of GNPs and GZ nanocomposites.....	54
4.7	Photoluminescence (PL) of GNPs and GNP-ZnO nanocomposites.....	56
4.8	Biocompatibility of GNP-ZnO nanocomposites .....	57
<b>5</b>	<b>Conclusions:</b> .....	<b>60</b>
<b>6</b>	<b>References</b> .....	<b>61</b>
<b>7</b>	<b>Plagiarism Report</b> .....	<b>66</b>

## List of Figures

Figure1.1: Flowchart of classification of composite material based on matrix .....	4
Figure1.2: Structure of graphene based nanocomposites a) Supported b) Encapsulated c) Incorporated d) Multilayered nanocomposites[8].....	6
Figure1.3: Single layer of graphene [28] .....	9
Figure1.4: Graphene building block for all other carbon allotropes. It can be rolled into (a) 0D buckyballs (b) 1D CNT (c)3D graphite in stacked form [29].....	10
Figure1.5: The electronic spin arrangement (a) elementary carbon and graphene b) Three $sp^2$ hybrid orbital of s and 2p orbital's of the 2nd orbit (c) Explanation of the orbital [30] .....	11
Figure1.6: (a) Hexagonal lattice (b) Two atom basis (c) Graphene 2D honeycomb lattice consist of two sub lattices A and B [34] .....	13
Figure1.7: Each unit cell contains one lattice point and two atom basis and each bravais lattice with two unit vectors $a_1$ and $a_2$ [35] .....	14
Figure1.8: First Brillouian zone of graphene reciprocal lattice [36] .....	15
Figure1.9: (a) A schematic diagram of Bernal AB stacking (b) A graphene bi-layer [37] ...	16
Figure1.10: The schematic representation of the different approaches for graphenesynthesis[54].....	17
Figure1.11: Image of Graphene nanoplatelets [56] .....	19
Figure 1.12: Unit cell of ZnO with cations and anions positions [62].....	21
Figure 1.13 Zinc interstitial sites in the ZnO wultzite lattice [62].....	22
Figure2.1: Diagram of XRD set-up[63].....	23
Figure2.2: X-ray diffraction from a crystal plane [64] .....	25
Figure2.3: Graphical representation of Field Emission Electron Microscopy (FESEM)[65]	27
Figure2.4: Schematic diagram of working principles of EDS [66] .....	29
Figure2.5: Band of functional group and finger print.....	30
Figure2.6: Diagram of FTIR set up [67].....	30
Figure2.7: A graphical representation of PL setup [68] .....	31
Figure2.8: Energy level diagram of Raman scattering[69].....	33
Figure2.9: Graphical representation of Raman Spectroscopy set-up[69].....	34

Figure2.10: The Process of DRS irradiated by light[70] .....	35
Figure2.11: Diffusion Reflectance spectroscopy set-up [71] .....	36
Figure3.1: Flow chart for Preparation of ZnO nanoparticles.....	40
Figure3.2:(a) Graphical representation of the formation of Graphene Nanoplateletsdecorated with ZnOnanoparticles(b) Flow chart for 10 wt % GNP-ZnO nanocomposites [72] .....	42
Figure3.3:Agar plate with disk surrounded by zone of inhibition [73] .....	43
Figure4.1: XRD pattern of pristine GNPs.....	44
Figure4.2:XRD pattern of pristine ZnO sample .....	45
Figure4.3: XRD patterns of pure GNP, pure ZnO NPs,10wt% GNP-ZnO, 15wt% GNPZnO,20wt% GNP-ZnO, 25wt% GNP-ZnO, 30wt% GNP-ZnO nanocomposites .....	47
Figure4.4: FESEM layout of (a) GNPs (b) 10wt% (c) 20wt% (d) 30wt% GNP-ZnO nanocomposites .....	49
Figure4.5: EDX spectra of (a) GNP (b) 10 wt % GNP-ZnO (c) 20 wt % GNP-ZnO (d) 30 wt % GNPZnO nanocomposites .....	51
Figure4.6: Raman spectra of (a) GNPs (b) 10 wt % GNP-ZnO (c) 20 wt % GNP-ZnO (d) 30 wt % GNP-ZnO nanocomposites.....	53
Figure4.7:FTIR spectra of (a)20 wt % GNP-ZnO(b)25 wt% GNP-ZnO(c)30 wt % GNP- ZnO nanocomposites .....	54
Figure4.8:DRS spectra of (a) Pure ZnO (b) 10wt% GNP-ZnO (c) 15wt%GNP-ZnO (d)20wt%GNP-ZnO(e) 25wt%GNP-ZnO(f) 30wt%GNP-ZnO(g) Pure GNP .....	55
Figure4.9: PL spectra of (a) Pure ZnO (b) 10wt%GNP-ZnO(c)20wt%GNP-ZnO (d) 30wt%GNP-ZnO nanocomposites.....	57
Figure4.10:Anti-bacterial activity of ZnO and GNP-ZnO nano-composites against MRSA and E.Coli bacteria.....	59

## List of Tables

Table 1-1: Classification of Graphene-inorganic nanocomposites [8] .....	5
Table 1-2: Different allotropes and its physical properties [33] .....	12
Table 1-3: Physical properties of GNPs [56] .....	18
Table 1-4: Basic physical parameter for ZnO [57] .....	20

<b>Abbreviation List</b>	
GNP	Graphene Nano platelet
GNPs	Graphene Nano Platelets
XRD	X-ray Diffraction
FTIR	Fourier Transform Infra Red
PL	PhotoLuminescence
DRS	Diffusion Reflection Spectroscopy
FESEM	Field Emission Scanning Electron Microscopy
EDX	Energy Dispersive X-ray Spectroscopy
EDS	Energy Dispersive Spectroscopy
UV-Vis	Ultra-Violet Visible Region
CNT/MWCNT	Carbon NanoTube/MultiWall Carbon NanoTube
GO/rGO	Graphene Oxide/Reduce Graphene Oxide
FBZ	First Brillouian Zone
CVD	Chemical Vapour Deposition
Cu, Mo	Copper, Molybdenum
SSA	Specific Surface Area
ZnO	Zinc Oxide
NPs	Nanoparticles
Å	Angstrom

## ABSTRACT

---

### Abstract

In this research work, GNP-ZnO nanocomposites samples have been synthesized by ex-situ method. These samples were prepared on different weight percentage GNPs loading on ZnO nanoparticles. The prepared GNP-ZnO nanocomposites were characterized by FESEM, EDX, X-ray Diffraction, Raman Spectroscopy, FTIR, PL and DRS. XRD measurements have shown that the GNP-ZnO nanocomposites have made and the diffraction peaks corresponding to GNPs and the wurtzite crystal structure of Zinc Oxide. The morphology of GNP-ZnO nanocomposites samples were investigated using FESEM and stoichiometry has been determined using EDX. The optical properties of GNP-ZnO nanocomposites have been analyzed with DRS and PL. In DRS the band gap is found to be varying from 3.34 to 2.24 eV with GNPs loading. The prepared GNP-ZnO nanocomposites have shown a powerful PL emission in the UV territory. The powerful emissions of GNP-ZnO nanocomposites have assigned to the radioactive recombination of electron occupying oxygen vacancies with a photo-excited hole. The bonding in nanocomposites was analyzed by Fourier Transform Infrared Spectroscopy. From the Raman spectra results, peaks had shifted towards the lower wave number with increasing GNPs loading on ZnO. The antibacterial property of GNP-ZnO nanocomposites have investigated against gram positive and gram negative bacterial and noted better inhibition zone than ZnO which is the significance of introduction of GNPs in GNP-ZnO nanocomposites.

## 1 Chapter No. 1 Introduction

No doubt that material science plays a key role in our lives, basically throughout the design, composition and fabrication of concerning new materials. Since from the Stone age to till now, our quality of life have become better over time with the introduction of current new materials. Materials are important to the science and technology because it is convenient to our lives for example cell phones, laptops, computers, touch screen and so on. Therefore the new materials grow up is the need of our society.

Our important feature for acquiring new material with enhanced properties is creative molecular design, preparation and synthesis of new materials. Nano-science emphasis not only on understanding the relationship between the arrangements of atoms, ions or molecules comprising a material but also on its overall physical properties & structure. Thus material science consists in the study of the structure and properties of existing materials, fabrications and characterization of new or improved materials and the use of characterization techniques to predict properties and structure of new materials that have not yet been made.

The developments of composites rest on carbon materials have drawn a lot of attention due to new materials with different structure and properties better than their constituents and previous composites systems with nanostructure materials. The shape, size and chemistry of the nanostructure materials produce composites that have a lot of potential in applications like sensors and actuators. Since breakthrough of graphene, graphene based composites also play a major role in the development of nano science and technology. In comparison with carbon nanotubes (CNTs), graphene has several advantages over CNTs. Graphene becomes unique due to its low density and high aspect ratio. The graphene shows exceptional physical properties which results in a most desired applicant for the evolution of graphene based composites.

### 1.1 Composites

Composites are prepared of two or more constituents materials. The constituent's material reveals different physical or chemical properties. Composite materials made out of constituents having properties totally different from their constituents. Due to the rareness in features; ceramics, metals and polymers are used in different applications. Further with these

extraordinary features, composites possess some restrictions, which limit their application in such a situation where multiple features are necessary. The beginning of engineered materials has improved the research significance. Presently composite materials contain many features such as durability, light weight, efficient electrical and thermal conductivity.

### **1.1.1 Basis of composite materials**

There are number of distinct parts in composites which are separated by the interfacial boundaries. To make property of the composites superior than their constituents, the appropriate amount of the constituents is evenly mixed. The large fraction of the composite material is called matrix whereas the lesser one is called reinforcement or filler. The filler are used to improve the functional properties of the matrix.

#### **1.1.1.1 Natural composite materials**

Organic materials are the basic constituents in the biological systems. These systems are composed of different materials contribute towards color, shape and smell. Biological systems can be attributed as natural composite materials. Wood is an example of natural composite made up of cellular fiber bonded together with lignin.

#### **1.1.1.2 Man made composite materials**

The utilization of materials in advance fields has enforced to build up materials with hybrid properties. Composites with different filler are being continuously developed to improve the mechanical, thermal and optical properties. Presently composites are being made and utilized in several advance applications. Man made composites are further classified on the basis of matrices

### **1.1.2 Classification of composites on the basis of matrices**

#### **1.1.2.1 Composite materials based on metal matrix**

Composites materials based on metal matrix consist of metals including (Mg, Al, Fe, Cu and Co etc) and embedded filler with ceramic phase including (carbides, oxides and nitrides etc) or metals. Metal based composites have high mechanical properties. Due to mechanical properties of both constituents high strength and particular modulus have been

obtained. From the last two decades their applications in aerospace and automotive have been increased [1].

#### **1.1.2.2 Composites materials based on ceramic matrix**

Composites materials based on ceramic matrix consist of a ceramic matrix and embedded filler with other ceramic substance. Ceramics have potential advantages over metals under high temperature situations such as low density, high strength and greater resistance to thermal oxidation. Ceramic based composites are still at early age of development as compared to metal and polymer based matrix [2].

#### **1.1.2.3 Composites materials based on polymer matrix**

Composite materials based on polymer matrix consist of a matrix like thermoset including unsaturated polyester, epoxies) or thermoplastic and embedded carbon, glass, steel or Kevlar fibers (dispersed phase). Strength, modulus and stiffness are weak for polymers but it can be made better by incorporating additives in thermoplastic and thermoset polymers. These composites have wide range applications due to light weight and high strength [3, 4].

#### **1.1.2.4 Composite materials based on graphene and chemically converted graphene**

Since graphene is hydrophobic in nature therefore the main limitation of graphene is its dispersibility. Graphene based composites are very important for many applications. The composite of distinctive properties of graphene, GO and rGO with those of other materials like organic or inorganic reagents reveal the new properties and scope of applications [5, 6].

Classification of composite materials based on matrix based is given below.

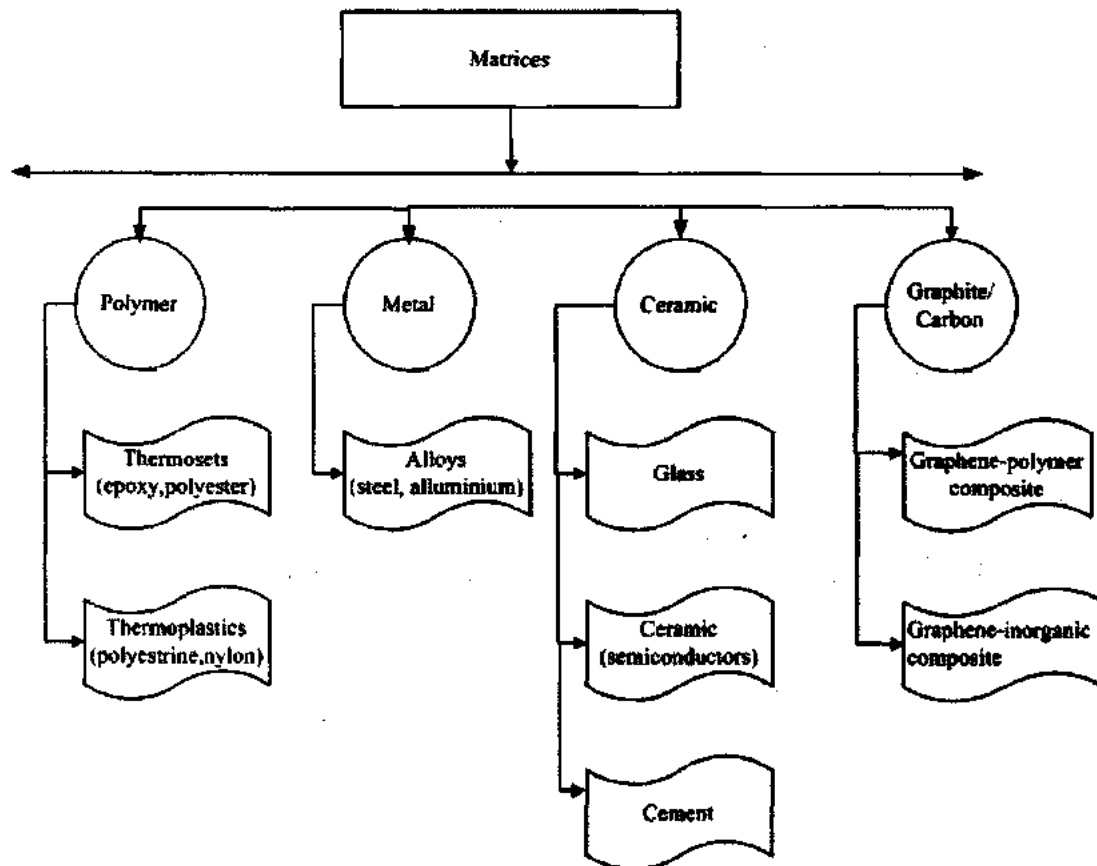


Figure 1.1: Flowchart of classification of composite material based on matrix

#### 1.1.2.4.1 Graphene /GO/rGO - inorganic nanostructures composites

Since graphene discovery, graphene-inorganic nanostructure composites (i.e. metallic and semiconducting nanoparticles) have been extensively studied due to their tested performances and potential applications in catalysis, optics and optoelectronics, super capacitors, fuel cells, batteries, bio/sensing etc. Inorganic composites refer to metallic nanoparticles such as noble metals: Pt, Au, Ag, Rh and Pd, and semiconducting nanoparticles like:  $\text{TiO}_2$ ,  $\text{ZnO}$ ,  $\text{SnO}_2$ ,  $\text{MnO}_2$ ,  $\text{Co}_3\text{O}_4$ ,  $\text{Fe}_3\text{O}_4$ ,  $\text{Fe}_2\text{O}_3$ ,  $\text{NiO}$ ,  $\text{Cu}_2\text{O}$ ,  $\text{RuO}_2$ ,  $\text{CdS}$  and  $\text{CdSe}$  [7].

#### 1.1.2.4.2 Graphene/GO/rGO - polymer composites

Graphene and chemically treated graphene with outstanding mechanical strengths, thermal stability, good conductivity and high surface area have been used as filler material for

polymer composites aiming the advancement of the electronic, mechanical and thermal properties of the polymer. The properties of graphene based polymer composites depends on the class of graphene, polymer as a matrix and the bonding or sandwiched between graphene and polymer. Graphene based polymer composites are classified into three classes [7]:

- Composites based on graphene filled polymer
- Composites based on layered graphene with polymer films
- Composites based on polymer with functionalized or chemically treated graphene

#### 1.1.2.4.3 Other graphene/GO/rGO – based composites

Other Composites based on graphene can be made by functionalization with organic crystalline, carbon nanotubes, metal-organic frameworks, fullerenes, biomaterials etc [7].

#### 1.1.3 Classification of graphene-inorganic nanocomposites

To classify new class of graphene-inorganic nanocomposites with respect to second constituents of the nanocomposites is given in Table 1.1

Table 1-1: Classification of Graphene-inorganic nanocomposites [8]

Graphene-inorganic nanocomposites	Types	Second Constituents
Graphene-Polymer nanocomposites		Polymers
Graphene-inorganic nanocomposites	Graphene-metal nanocomposites	Metal
	Graphene-carbon nanocomposites	Carbon building Block
	Graphene-metalcompound nanocomposites	Metal compound
	Graphene nonmetal nanocomposites	Non-Metal

#### 1.1.4 Classification of nanocomposites based on structure

The classification with respect to the supporting constituent has its own limitation if two or more constituents were mixed in nanocomposites. Thus in accordance to different structures, graphene based nanocomposites are categorized into four classes depicted in Figure. 1.2.

- supported nanocomposites
- encapsulated nanocomposites
- incorporated nanocomposites

- multilayered nanocomposites

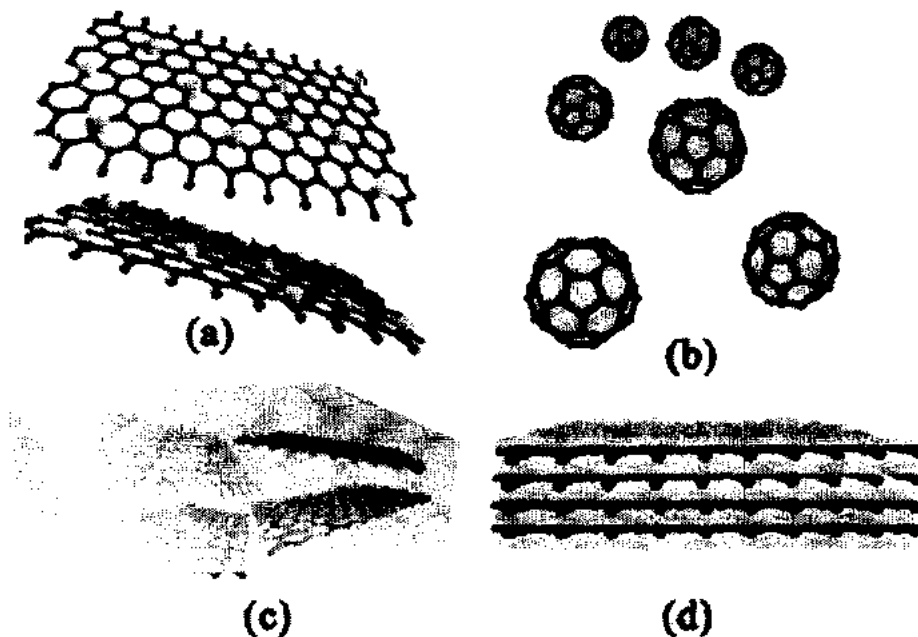


Figure 1.2: Structure of graphene based nanocomposites a) Supported b) Encapsulated c) Incorporated d) Multilayered nanocomposites [8]

### 1.1.5 Applications of graphene inorganic nanocomposites

Graphene blended with different inorganic nanostructures using different structural units and fabrication methods constitute new class of materials. The graphene–inorganic nanocomposites mostly maintain the appropriate properties of graphene and the inorganic nanostructures. It also significantly improves the inherent characteristic because of combined effect of both constituents. The superior function of graphene-inorganic based nanocomposites in catalysis, solar cells, energy storage and sensors applications are discussed below in detail.

#### 1.1.5.1 Catalysis

Nanostructures of Carbon (C) possess large surface area, good thermal and electrical properties, easy modification, high chemical inertness and low price. Therefore it is generally acting as immobilizing catalyst in reactions. Similar to other SWCNT and MWCNT catalysts,

the graphene and inorganic based nanocomposites are also considered to be brisk catalysts in photochemical, wet chemical and electrochemical reactions [9].

#### **1.1.5.2 Photo catalysis**

Photo catalysis can be defined below. When the photons interact with the photo catalyst having photon energy equal or greater than the material band gap, As a result electron-hole pairs are created whose further interaction result in the production of hydrogen and hydroxyl ions and able to undergo secondary reactions. This results in disintegration of organic toxic waste and degradation of large metal ions.

But in the photo catalysis process, the sudden recombination of photo created electron hole pair reduces the effectiveness of photo catalyst. Therefore, the electrons-hole pair recombination can be minimized due to good electrical property of graphene. In this case, it can be used for electron transfer to improve the photo conversion effectiveness of the photo catalytic materials [10].

#### **1.1.5.3 Energy storage and conversion**

In the recent years, there is enormous increase in the global demand for energy which has inspired significant effort for the progress of energy storage. For this purpose, graphene based material have been used as electrodes in energy storage devices. It may possible only due to excellent electrical properties, large surface area and good chemical stability. In recent times graphene inorganic nanocomposites have been used in fuel cells, solar cells, super capacitors and in energy storage/conversion devices [11, 12].

#### **1.1.5.4 Solar cells**

Solar cells change the energy of sun light into electricity through photovoltaic effect. Since graphene has excellent electrical and optical properties with respect to high electron mobility, graphene-inorganic nanocomposites have come out as one of the interesting electrode materials for solar cell applications. These applications can be dye-sensitized solar and quantum dot-sensitized solar cells. Nowadays dye-sensitized solar cells have drawn great attention due to steady light conversion into electricity performance, low cost and easy fabrication [13].

#### 1.1.5.5 Fuel cells

These are such devices which involve electro-catalyst at the anode while oxygen reduction (OR) at the cathode to produce desired electricity. For this purpose graphene–inorganic nanocomposites show outstanding electro-catalyst facilitation, which renders its application in fuel cells for the next-generation, for example graphene–Pt nanocomposites in methanol fuel cells and graphene–Pd nanocomposites in direct carboxylic acid fuel cells [14, 15, 16]

#### 1.1.5.6 Gas detector

Gas detector is a device that detects the presence of gases, it is also called gas sensor. CNT based detectors have drawn a lot of attraction for the researcher from the last few years due to fast detection of different gas molecules. Nowadays due to good properties of graphene as compared to CNTs [17], some researchers have studied sensitivity for the detection of H<sub>2</sub> [18], H<sub>2</sub>S [19], propanal [20], ethanol [21] and NO<sub>2</sub> [22] molecules by using graphene-inorganic nanocomposites as gas sensor materials.

## 1.2 History of Graphene

Marița culture implement graphite just as a ceramic paint to furnish pottery in southeastern Europe and its use can be traced back to the 4th millennium B.C [23]. P.R.wallace has used the tight binding model to study the band theory of graphite in 1947 and assumed that conduction happens only in one layer of graphite which is graphene layer [24]. Graphene sheet was first synthesized by Benjamin C. Brodie in 1859 [25] and changed into graphene oxide sheet. Further it was modified by Hummers and Offeman in 1957 [26]. Until 2004, Andre Geim and Konstantin Novoselov reported the first experimental breakthrough of graphene [27] and both won the 2010 Noble prize in physics for this remarkable discovery. Graphene layer is shown in Figure 1.3 [28]

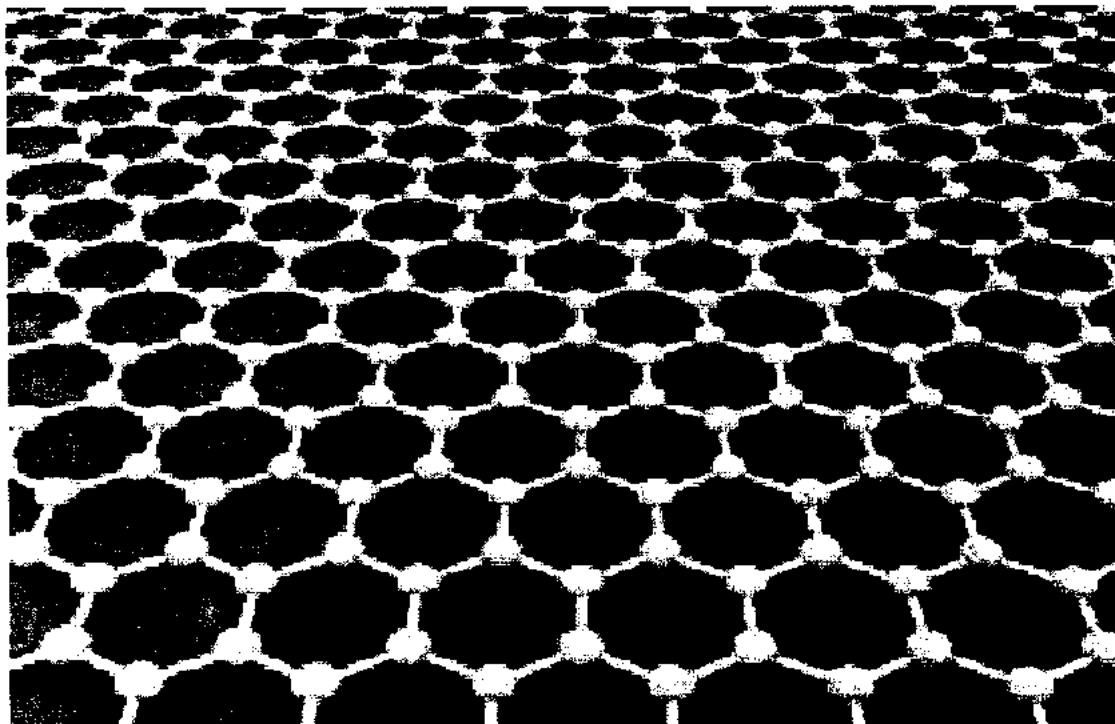


Figure 1.3: Single layer of graphene [28]

### 1.2.1 Carbon Allotropes

Graphene is a single planar sheet of carbon atoms where all the carbon atoms form covalent bonds and packed tightly into 2D (two dimensional) honeycomb crystal lattice. Graphene is a fundamental building block for graphite materials of all dimensions as shown in

Figure 1.4 [29]. Graphene is also considered to be the mother of all graphite form materials. It can be wrapped up into a sphere producing buckyballs (0D), folded into a cylinder create carbon nanotubes (1D) and arranged in a stack to produce graphite (3D).

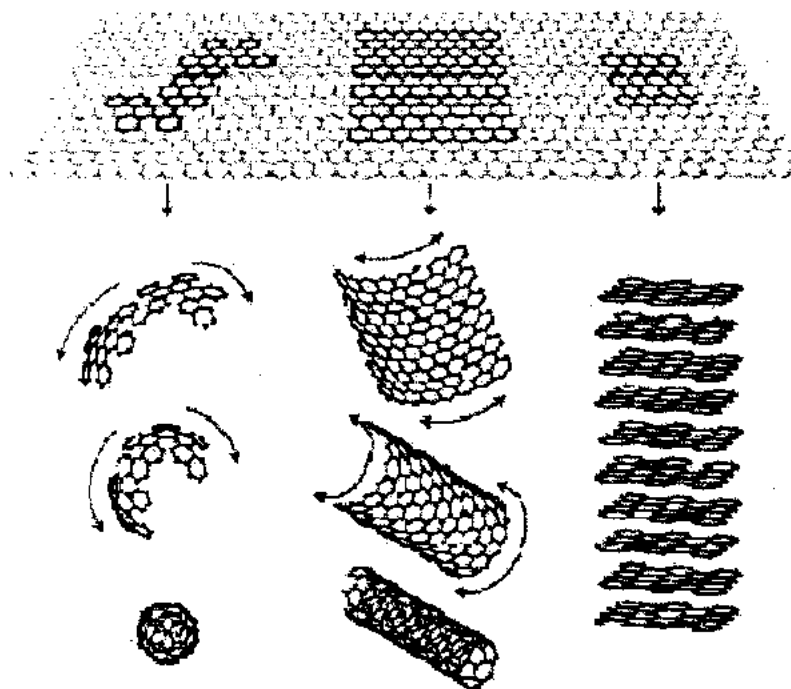


Figure 1.4: Graphene building block for all other carbon allotropes. It can be rolled into (a) 0D buckyballs (b) 1D CNT (c) 3D graphite in stacked form [29]

### 1.2.2 Graphene hybridization and bonding

Carbon is a group IV element of the periodic table and chemically very active to interact with other molecules to form different compounds and crystalline materials. Carbon element has four valence electrons in its outermost shell which have a propensity to interact with each other to form different types of carbon allotrope. Basically in carbon element, the four valence electrons are configured in 2s and 2p orbital's as shown in Figure 1.5 [30].

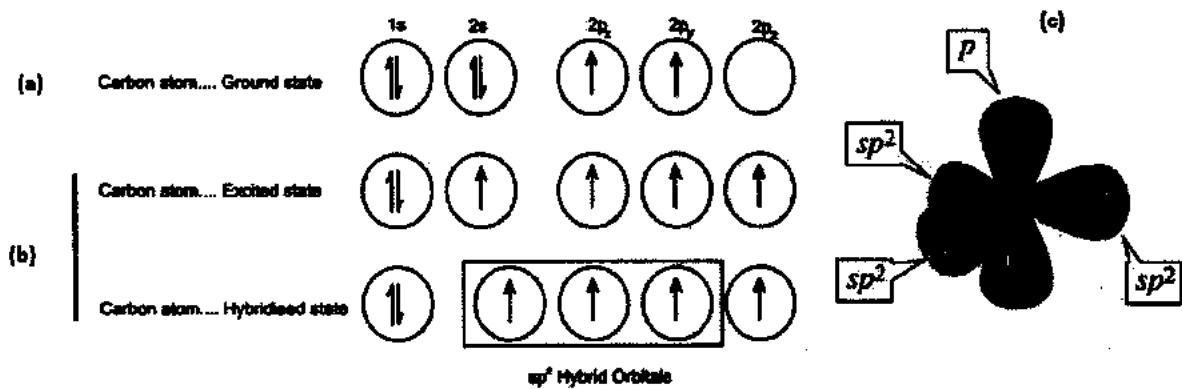


Figure 1.5: The electrons and their relative spin arrangement (a) elementary carbon and graphene (b) Three  $sp^2$  hybrid orbital of s and 2p orbital's of the 2nd orbit (c) Explanation of the orbital [30]

When carbon atoms form a crystal then one of the 2s electron gained energy from the neighboring nuclei and jumped to the  $2p_z$  orbital [31, 32]. This type of bonding or interaction occurs in between the 2s and 2p orbital of carbon atoms. This type of interaction of atomic orbital is called hybridization and the new orbitals are termed as hybrid orbitals. Due to multiple type of hybridization, carbon shows different allotropes as shown in Table 1.2 [33].

In  $sp^2$  hybridization of graphene, each carbon atom is bonded covalently with three other carbon atoms in the plane and the angle between consecutive bonds is  $120^\circ$ . These three covalent bonds are termed as  $\sigma$ -bonds; which connect carbon atoms into a honeycomb lattice and responsible for strong mechanical properties of graphene. The  $2p_z$  electron builds a bond called  $\pi$ -bonds which is allocated perpendicular to the plane. The  $2p_z$  electrons are loosely connected to nuclei and thus are easily delocalized. These delocalized electrons are important for electronic properties of graphene.

Table 1-2: Different allotropes and its physical properties [33]

Dimensions	0D	1D	2D	3D	3D
Allotropes	C <sub>60</sub> Bucky Ball	Carbon nanotubes	Graphene	Graphite	Diamond
Color	Black Solid	Black	Black	Black to Grey	Colorless
Density	1.7-1.9 g/cm <sup>3</sup>	2g/cm <sup>3</sup>	>1g/cm <sup>3</sup>	1.99-2.3g/cm <sup>3</sup>	3.52g/cm <sup>3</sup>
Hybridization	sp <sup>2</sup> trigonal planar	sp <sup>2</sup> trigonal planar	sp <sup>2</sup> planar sheet	sp <sup>2</sup> trigonal planar	sp <sup>3</sup> tetrahedral
Electronic Properties	Semi-Conductor	Metal/Semi	Semi-metal	Metal	Insulator
Crystal Structure	Truncated icosahedron	Cylindrical	Honeycomb	Tabular	Cubic

### 1.2.3 Crystal Structure

The 2D honeycomb lattice is not a bravais lattice because two neighboring sites A and B are in-equivalent. However honeycomb lattice is still a lattice because it consists of a repeating unit cell and as a result non-bravais lattice can be converted to bravais lattice in a honeycomb lattice considering grouping of points A and B together and the resulting lattice as shown in Figure 1.6 [34] which is now a bravais lattice with a basis of A-B. Thus each bravais lattice point shows two crystal lattice points. In solid crystals, the points are position of atoms and the basis is understand as the number of atoms grouped together at each bravais lattice point.

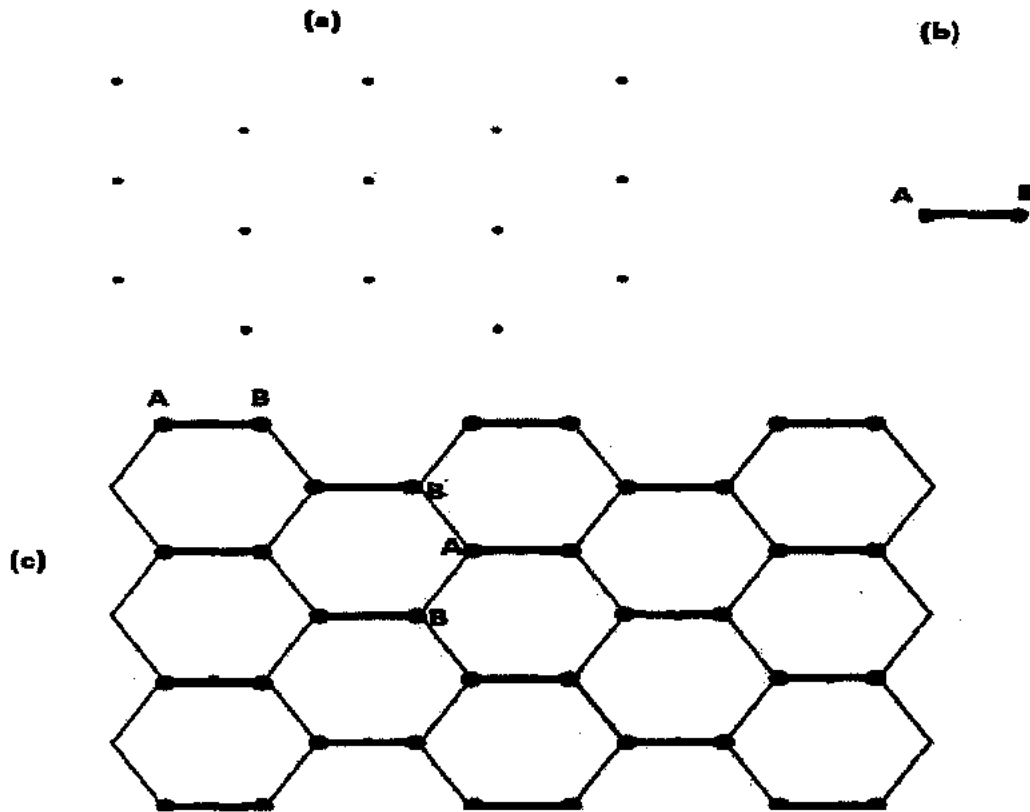


Figure 1.6: (a) Hexagonal lattice (b) Two atom basis (c) Graphene 2D honeycomb lattice consist of two sub lattices A and B [34]

It is quite clear that the graphene structure consist of two sub lattices, A (green color point) and B (Red color point), with each Bravais lattice having primitive lattice vectors denoted as  $a_1, a_2$  given by in Figure 1.7 [35].

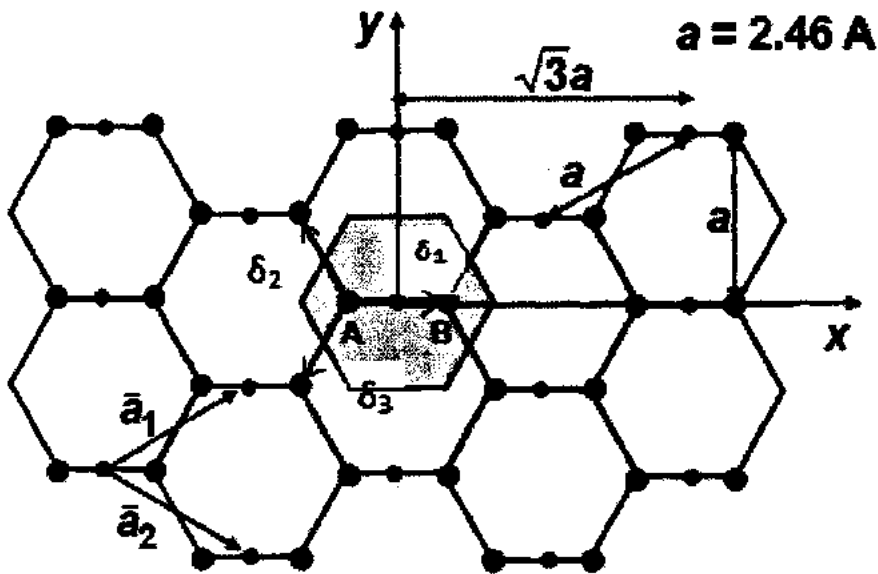


Figure 1.7: Each unit cell contains one lattice point and two atom basis and each bravais lattice with two unit vectors  $a_1$  and  $a_2$  [35]

$\bar{a}_1$  and  $\bar{a}_2$  vectors in translation form are given below

$$\bar{a}_1 = a \left[ \frac{\sqrt{3}}{2} \bar{x} + \frac{1}{2} \bar{y} \right] \quad (2.1)$$

$$\bar{a}_2 = a \left[ \frac{\sqrt{3}}{2} \bar{x} - \frac{1}{2} \bar{y} \right] \quad (2.2)$$

In simplified form we can write as

$$\bar{a}_1 = \frac{a}{2} (1, \sqrt{3}), \quad \bar{a}_2 = \frac{a}{2} (\sqrt{3}, -1) \quad (2.3)$$

Lattice vectors from A sub-lattice atom to the three nearest neighbor B sub-lattice atoms, can be expressed as;

$$\delta_1 = \frac{a}{2} (1, \sqrt{3}) \quad (2.4)$$

$$\delta_2 = \frac{a}{2} (1, -\sqrt{3}) \quad (2.5)$$

$$\delta_3 = -a(1, 0) \quad (2.6)$$

Where  $a = 0.14 \text{ nm}$  is the adjacent spacing between two carbon atoms.

The reciprocal lattice vectors  $b_1, b_2$  represented by the condition  $a_i \cdot b_j = 2\pi\delta_{ij}$ , will be as

$$b_1 = \frac{2\pi}{3a}(1, \sqrt{3}), b_2 = \frac{2\pi}{3a}(1, -\sqrt{3}) \quad (2.7)$$

Where  $\delta_{ij} = 0$  if  $i \neq j$  and  $\delta_{ij} = 1$  if  $i = j$

### 1.2.4 Brillouian zone

First Brillouian zone of the reciprocal lattice is defined in typical manner, as the region enclosed by the planes bisecting the vectors to the nearest reciprocal lattice points which results in an FBZ of the same form as the original hexagons of the honeycomb lattice, but rotated by  $90^\circ$ . The six points at the corners of the FBZ can be categorized into two groups of three which are equivalent, so we should consider only two in-equivalent corners  $K$  and  $K'$ , as shown in the Figure 1.8 [29]. These are called Dirac points and their positions in  $k$ -space can be denoted as;

$$K = \frac{2\pi}{3a}\left(1, \frac{1}{\sqrt{3}}\right), K' = \frac{2\pi}{3a}\left(1, -\frac{1}{\sqrt{3}}\right) \quad (2.8)$$

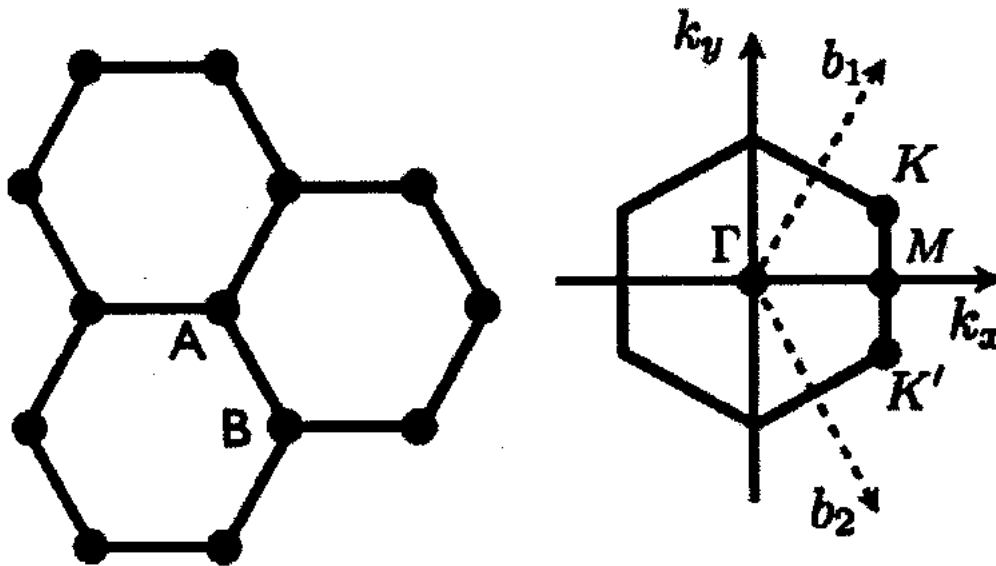


Figure 1.8: First Brillouian zone of graphene reciprocal lattice [36]

### 1.2.5 Graphite and Bi-layer graphene

Three dimensional graphite structures are formed when several graphene sheets are layered on top of each other. It results in hexagonal structure with four atoms per unit cell and the dimensions are  $c = 6.71 \text{ \AA}$  and  $a = 2.45 \text{ \AA}$ . The two-dimensional hexagonal lattices are

stacked, either in an ABAB pattern or an ABCABC pattern. The ABAB stacking of graphene forms Bernal AB-stacking while ABCABC pattern form rhombohedral structure. In Bernal AB-stacking the A sub-lattice of one graphene layer is linear on top of B sub-lattice of the other graphene layer. The ABAB pattern is also called Bi-layer graphene and shown in Figure 1.9 [37].

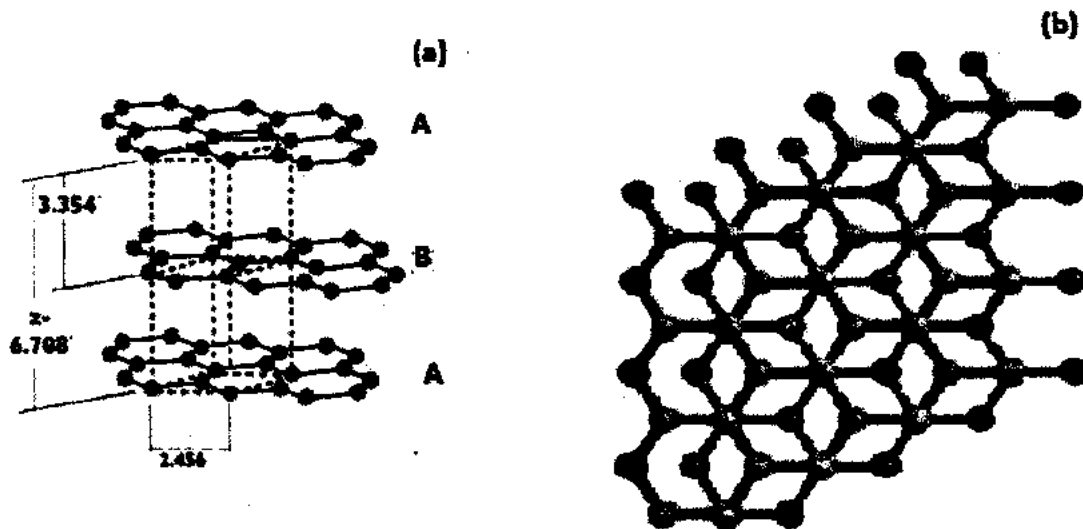


Figure 1.9: (a) A schematic diagram of Bernal AB stacking (b) A graphene bi-layer [37]

### 1.2.6 Properties and application of graphene

Due to remarkable properties of graphene, it becomes a rising star for the researchers and its applications are significant in different areas of life. Graphene make a superior candidate for the semiconductor devices due to its high electron mobilities along the plane i.e.  $15,000 \text{ cm}^2 \text{ V}^{-1} \text{ s}^{-1}$ , am-bipolar field effect [38,39]. Apart from the tremendous high charge carrier mobilities, graphene is also a good candidate for photovoltaic devices [40-41], since it absorbs only 2% of light and independent of wavelength across the visible spectrum [42]. Conducting films for display, touch screen and solar cell have been made from graphene [43-46]. Due to large planar surface and low electrical noises of graphene field effect transistor make use in optoelectronics and sensor applications [47-50]. The high mechanical properties and flexibilities of graphene are highly helpful in electrochemical devices [51]. In electronics, a cutoff frequency of 100GHz for a graphene field effect transistor of 240nm gate length has been achieved which is higher than

silicon transistor of the same gate length [52]. There is a vast potential and speedy advancement in research due to novel properties of graphene and graphene composites and will soon beginning to influence industry [53].

### 1.2.7 Synthesis methods of graphene

Synthesis methods of graphene consist of two main classes: the top down and bottom up approach and are summarized in the scheme bellow

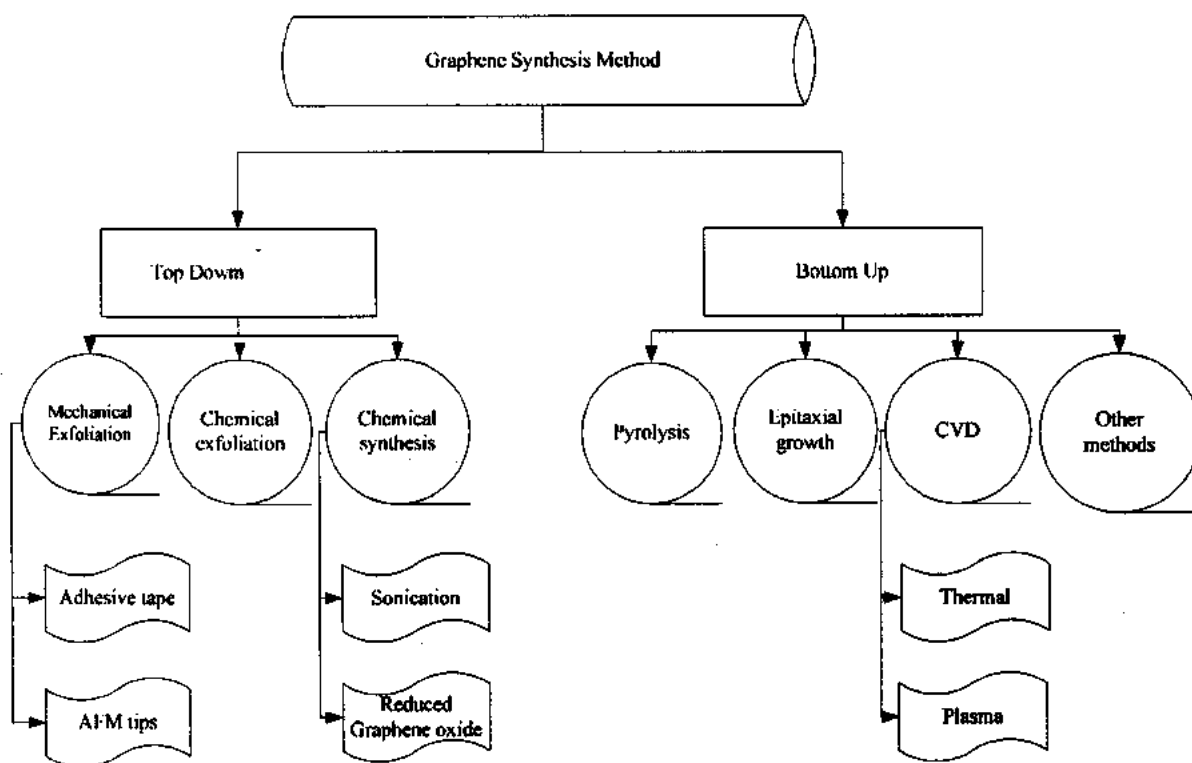


Figure 1.10: The schematic representation of the different approaches for graphene synthesis [54]

### 1.2.8 Graphene nanoplatelets

Graphene nanoplatelets are neither graphene nor graphite but it is the intermediate stage between graphene and graphite. It has different synonym names in literature like nano graphene platelets (NGP), graphite nanoplatelets (GNPs), multilayer NGP, graphene flakes and nano-scaled graphene powder etc. Its surface area is twice than CNT [55]. Graphene nanoplatelets are composed of about one to hundreds of atomic layers thickness in “platelet” morphology. It can be synthesized with low cost and obtain with high purity and performance. GNP has high aspect

ratio of thickness to width with excellent electrical, thermal conductivity and mechanical properties. It has been divided into different grades with respect to SSA and named Grade H, Grade M and Grade C. The following synthesis methods are used for GNP.

- Mechanical exfoliation of graphite
- Oxidation of graphite oxide
- Direct intercalation and exfoliation

### 1.2.9 Why use GNPs

Since graphene preparation is difficult, complex and economically costly whereas graphene nanoplatelets (GNPs) are more easily to obtain and having same properties as graphene and also can be used in the same applications. Physical Properties of GNP is shown in Table 1.3 [56].

Table 1-3: Physical properties of GNPs [56]

Parameters	Values
Appearance	Black Powder
Diameter	20-50 $\mu$ m
Thickness	<100nm
Carbon content	>99.5wt%
True density	$\sim$ 2.25g/cm <sup>3</sup>
Thermal conductivity	$\sim$ 3000W/mK
Tensile strength	$\sim$ 1000Gpa
Young's Modulus	$\sim$ 1060Gpa

### 1.2.10 Applications

GNP is considered to be ideal for applications due to excellent properties just as strengthening composites materials, forceful as barriers, ultra capacitor electrodes, anode materials for lithium-ion batteries, substrate for active materials and super capacitors etc. It has not found any serious drawbacks at current time. The GNP image is shown in Figure 1.11 [56].

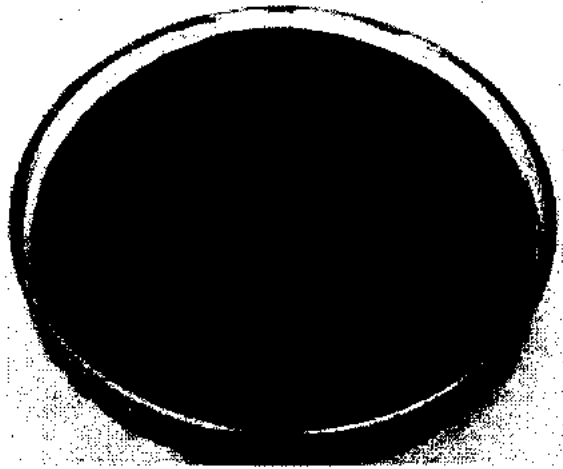


Figure 1.11: Image of Graphene nanoplatelets [56]

### 1.3 Zinc Oxide (ZnO)

ZnO crystal structure occurs in three shapes; hexagonal wurtzite, cubic rock salt and cubic zinc blende. The hexagonal wurtzite structure is most common and stable at ambient conditions. The zinc blende cubic structure can be sustained by growing ZnO on substrate. The rock-salt structure can be observed at high pressure approximately 10GPa.

ZnO crystal is an inorganic compound also known as zincite and hardly exists in nature. It appears white in color and almost unsolvable in water. Maximum zinc oxide used commercially and is created un-naturally. ZnO is a transparent direct band gap with 3.37eV of the II-VI semiconductor group. It has some favorable properties like broad band gap, good transparency, high room temperature and luminescence etc.

Table 1-4: Basic physical parameter for ZnO [57]

Parameters	Values
Stable Phase at 300 K	Wurtzite
Density	5.606g/cm <sup>3</sup>
Melting point	2248K <sup>0</sup> , 1975C <sup>0</sup>
Band gap	3.34eV
Excitation Binding Energy	60meV
Young Modulus	106.5GPa, 115.9GPa
Refractive Index	2.008, 2.029
Thermal Conductivity	0.6, 1-1.2
<b>Lattice Parameters</b>	
a	3.2496Å
c	5.2096Å
c/a	1.602

#### 1.3.1 ZnO structure

ZnO has most stable wurtzite crystal structure which has hexagonal close-packed (HCP) lattice type. This structure belongs to  $P63mc$  space group [58]. It is distinguished by two interconnected sub lattices of  $Zn^{2+}$  and  $O^{2-}$ . In this case each cation is surrounded nearby four anions at the edges of tetrahedron symmetry with a  $sp^3$  covalent bonding and vice versa. From

Various shapes of ZnO lattices, the wurtzite has been reported to be the most thermodynamically stable phase [59]. Tetrahedral uniformity is found to have significantly role for the polarity of ZnO. It appears along c-axis of the hexagonal. The polar symmetry of ZnO is strongly dependent on the spontaneous polarization and piezoelectricity [60]. This structure has number of alternating planes which are formed tetrahedrally coordinated  $O^{2-}$  and  $Zn^{2+}$  ions. This stacking of planes is along the c-axis as depicted in Figure.1.12 [62]. There are positively charged (0001)-Zn and negatively charged (0001)-O polar planes. This oppositely charged ions packing along c-axis leads to spontaneous polarization divergence in surface energy and normal dipole moment [61]. These polar planes are more safe and stable than non polar planes. ZnO is naturally n-type semiconductor material due to existence of point defects in structure. These point defects are mostly created in ZnO due excess of zinc interstitial and vacancy defects in ZnO matrix. These surplus and excess zinc atoms in ZnO acts as donor interstitials which lead to n-type conductivity. In ionic structure, the excess Zn occurs as  $Zn^{+}$  interstitials that are movable and they have trend to hold unique interstitial sites with Miller index  $(\frac{1}{3}, \frac{2}{3}, 0.875)$  as shown in Figure.1.13 [62].

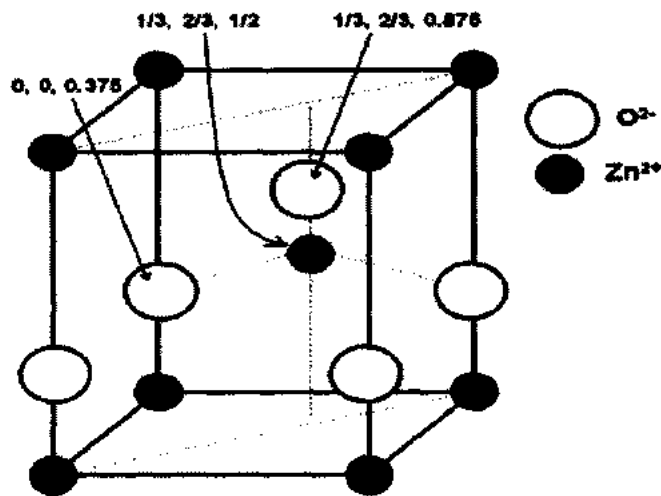


Figure 1.12: Unit cell of ZnO with cations and anions positions [62]

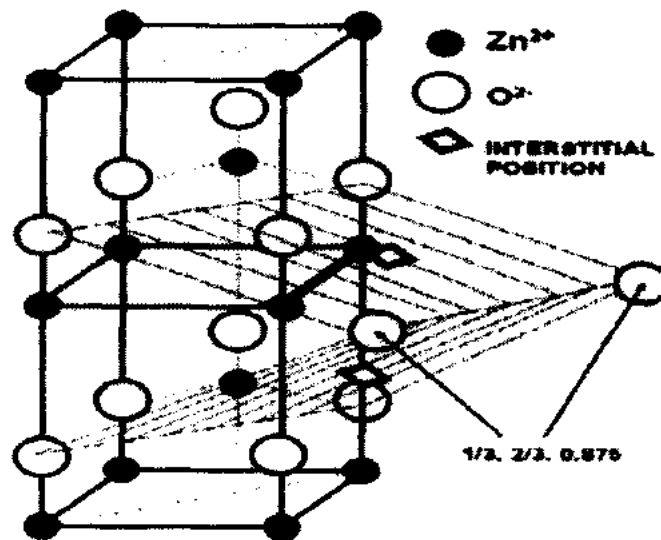


Figure 1.13 Zinc interstitial sites in the ZnO wurtzite lattice [62]

### 1.3.2 Applications

- The ZnO is potential for heat-protecting windows, light emitting diodes and liquid crystal displays
- ZnO is used in thin film transistors, ceramics plastic and circuit's amplifiers.
- ZnO is also used in UV light emitters, transparent electronics, chemical sensors and piezoelectric devices.
- ZnO is biocompatible material and used in antibacterial and cosmetic lotions

These outstanding physical properties act as the basis for motivation in our research for fabrication of ZnO based graphene nanocomposites to further improve physical characteristic of ZnO.

## 2 Chapter No.2 Analytical Techniques

Characterizations are being used to analyze and examine the properties of nanostructured materials. Therefore it is necessary to understand the working principles and instrumental detail of the characterization techniques, for example Field Emission Scanning Electron Microscopy (FESEM), X-Ray Diffraction (XRD), Raman spectroscopy, Energy Dispersive Spectroscopy (EDS), Fourier Transform Infrared Spectroscopy (FT-IR) and Photoluminescence (PL).

### 2.1 X-ray Diffraction (XRD)

#### 2.1.1 Introduction

Among different characterization techniques, XRD is the most useful technique for examine the structure of material. It is a non destructive tool and is used to get information about different crystalline materials of the examined sample by diffraction pattern. XRD can analyze samples both in powder as well as in solid forms. XRD pattern is based on regular arrangement of atoms or in materials. XRD set up is shown in Figure 2.1[63]

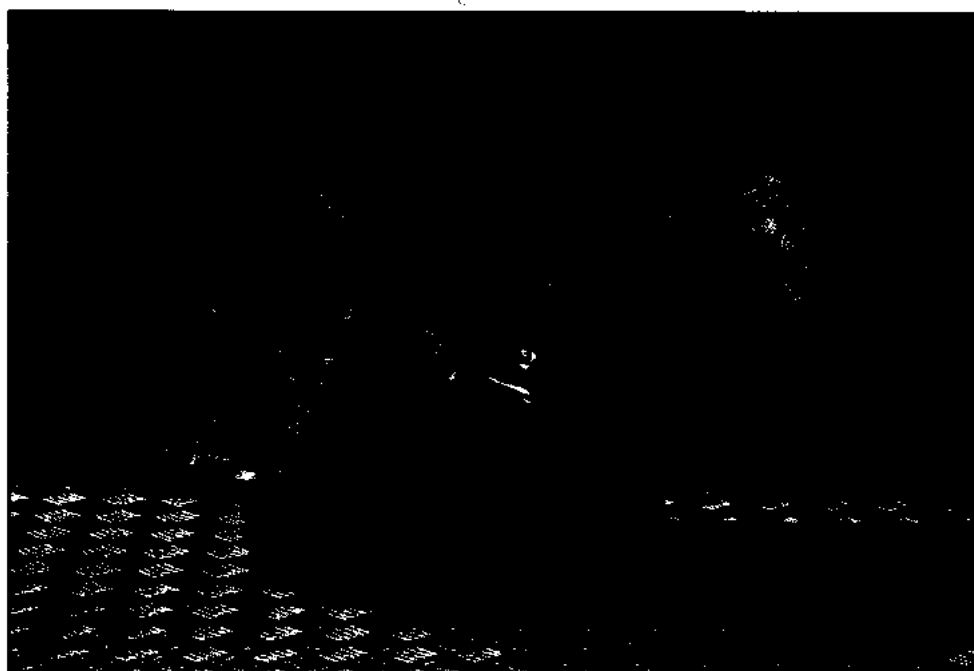


Figure 2.1: Diagram of XRD set-up [63]

Diffraction occurs only when waves interact with arranged structure of material at comparative scale. In XRD, if the atomic distance of the crystal plane is comparable to the wavelength of x-rays then diffraction will occur as a result of interference of diffracted x-ray from the crystalline planes. Since XRD is based on x-rays, therefore it is necessary to understand the nature of x-rays.

### 2.1.2 X-rays

X-rays are form of electromagnetic radiation with high energy penetrating rays. This was discovery of German physicist Roentgen in 1895. These radiations have wide application in the field of material science, engineering and medical. Only in material science it has a lot of utilization for material analyses such as XRD, X-ray Fluorescence (XRF) and x-ray photoelectron spectroscopy (XPS). For diffraction applications, only short range wavelengths of x-rays close to  $0.1\text{\AA}$  are used. The x-rays are able to penetrate into the matter and display data relevant to the structure of the matter.

X-radiation are generated in an x-ray tube when a beam of electron produced by heating filament and accelerated towards an immobile or rotating rigid target across a high potential. X-rays have two types continuous x-rays and characteristic x-rays. In continuous x-rays, the electrically charged particles of sufficient energy are decelerated which results in x-rays release called Bremsstrahlung radiations. In characteristic x-rays the electrons are released from the innermost orbit of target atoms by the ionization process, then an electron from the outermost orbit jump into inner orbit and fill the vacancy at which it was created, the x-ray emitted is called characteristic x-ray and it is the property of the target material. The targets in x-ray tubes are commonly Cu or Mo. As we know that photon is a particle of electromagnetic radiation and the relation between photon energy and frequency is given by equation

$$E = hf \quad (2.1)$$

$$\text{Since } c = f\lambda \text{ and } f = \frac{c}{\lambda}$$

Therefore

$$E = \frac{hc}{\lambda} \quad (2.2)$$

Where  $h$  is Planck's constant,  $\lambda$  wavelength of the X-ray and  $c$  the speed of light.

### 2.1.3 Bragg's Law

In 1912 W. L. Bragg physicist first proposed a law about diffraction known as Bragg's Law. The Bragg's Law is a basic in the determination of crystal structure and important step in the field of x-ray crystallography.

When the sample is exposed to x-rays beam, then each atom of the plane act as a source of a coherent scattered wave. The scattered waves from one plane atoms will interfere with the waves from other surrounding plane atoms and will result in a constructive or destructive interference depending upon the path difference of diffracted x-rays. This interference is shown in Figure 2.2 [64].

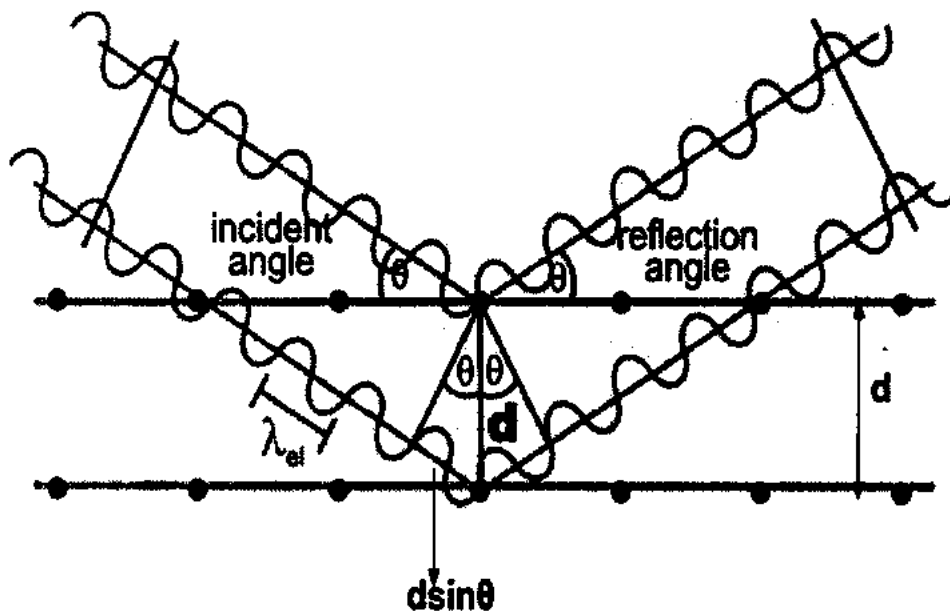


Figure 2.2: X-ray diffraction from a crystal plane [64]

The condition for diffraction of the incident radiation is given in equation below

$$2d_{(hkl)} \sin \theta = n\lambda \quad (2.3)$$

Where  $d_{(hkl)}$  is the distance between atomic planes,  $\lambda$  is the wavelength of the x-ray,  $\theta$  is the angle of incidence and  $n$  is the order of reflection. The Bragg Law is a result of periodicity of the space lattice.

## 2.2 Field Emission Electron Microscopy (FESEM)

### 2.2.1 FESEM working

In FESEM, electrons are emitted from field electron emitter which act as electron gun source and accelerated in a high vacuum column tube. The primary electrons are deflected and focused by electronic lens to produce narrow beam that interact with sample. As a result of interaction, secondary electrons are released from the sample. These secondary electrons have close relation to the surface structure of the sample and collected in a detector to produce an electronic signal. This signal is amplified and processed further to be seen on computer screen. The diagram of FESEM is shown in Figure 2.3 [55].

### 2.2.2 Vacuum

FESEM composed of two vacuum pumps which develop vacuum in a column tube up to  $10^{-5}$  torr to permit primary electron movement along the tube without scattering and are allowed to target sample.

### 2.2.3 Field Emission Source

Actually Field emission source is an electron gun which is operated at kilovolts negative potential with respect to adjacent electrode. The source are either made of tungsten or coated with zirconium oxide called schottky type. The electrons are expel when the field emission source are heated and producing a clear image, less electrostatic distortions and spatial resolution  $< 2\text{nm}$ . Due to this emitter source, FESEM and others scanning microscopes are differentiated.

### 2.2.4 Anode

FESEM composed of two anodes for the electrostatic focusing. The potential difference exists between the first anode and the field emission tip which is acquired to keep in control of the current emitted from the field emission tip. This potential difference is called extraction

voltage. The voltage called accelerating voltage between cathode and second anode can be used to increase velocity and enhances the electrons beam energy in to the column. This accelerating voltage combines with diameter of beam having capacity to separate the two type of sample which is strictly close with each other.

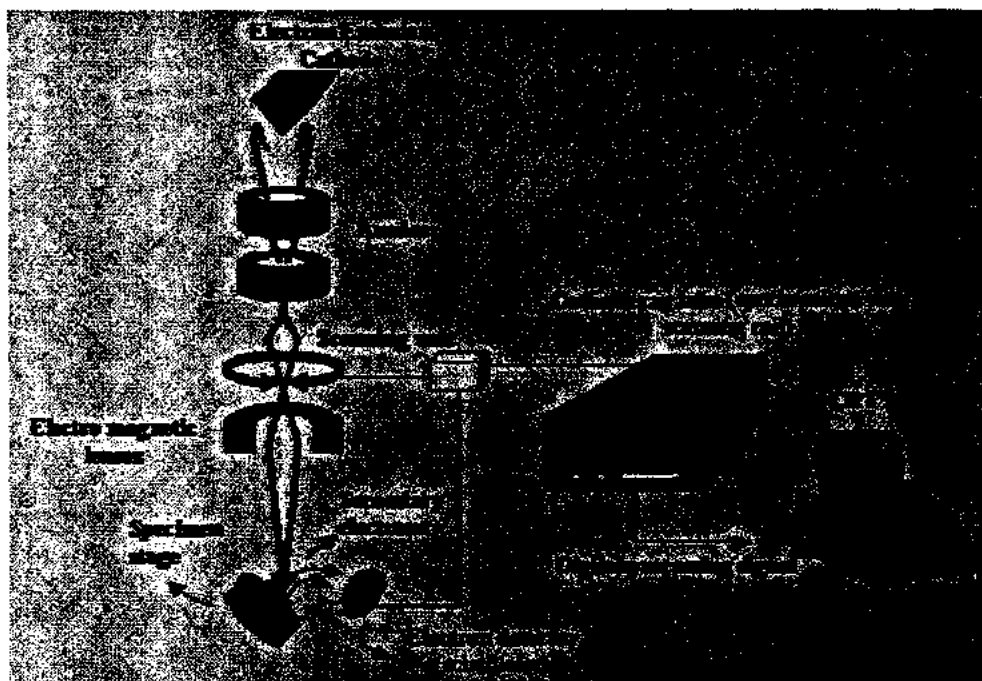


Figure 2.3: Graphical representation of Field Emission Electron Microscopy (FESEM) [65]

### 2.2.5 Electromagnetic Lenses

Electromagnetic lenses make FESEM highest resolution instrument. To resolve feature on the sample surface, the beam diameter should be smaller than feature. Therefore to condense electron beam, the electromagnetic lens are used for image processing.

### 2.2.6 Depth of Field

In microscopy, Depth of the field is an important factor and characterizes the potential to concentrate the large change in the sample topography. Long working distance in column and small aperture generate the image appearance in a focus over large change in Z-axis. A particular current specified to objective lenses, the sample moves upright until it becomes focus.

### 2.2.7 Electron beam and sample interaction

The electron beam interacts elastically and in-elastically with specimen and allowing various forms of signals. In elastic interaction, electron beam kinetic energy is not altered and the electron path is affected only. While in inelastic interaction, the electron gives some energy to the atoms of the sample and as a result the electron with loss in energy changes in small trajectory divergence. The signal created by this way named secondary electron (SE), X-Rays and Auger electrons. Each of these signals gives the information about topography, surface characteristic, crystallography, and composition of the sample.

### 2.2.8 Applications

- FESEM produces clear, less electro-statically distorted images and 4 to 6 times better than conventional SEM.
- Smaller area of the sample can be investigated at electron accelerating voltage than EDS.
- It uses ultra high magnification

## 2.3 Energy-Dispersive Spectroscopy (EDS)

EDS is used to study the elemental composition and their relative proportion in atomic percent of the nanostructure samples. This method includes the interaction between specimen and high energy electrons ( $> 200$  keV) which penetrate through materials and knock out electron from inner shell of the atom and creates vacancies. In order to fill this vacancy, electron will jump from outer shell into lower shell of the atom and will emit characteristic x-rays which will be detected by the detectors. This technique is related to basic principle that each element has unique atomic structure and permit x-rays of its own family which are distinguished from other elements. In other words EDS based on Moseley law for elemental analysis. According to Moseley law "the energy of characteristic radiation with in a series of lines varies with atomic number". Generally the EDS set up is attached with SEM system.

EDX spectrum gives broad range information of the elemental composition of the materials. The EDX spectrum peaks correspond to energy level and show information with respect to the element for which the peak x-ray has been noted. The intensity of peak of certain

elements in a spectrum corresponds to the elemental concentration of that element in the material.

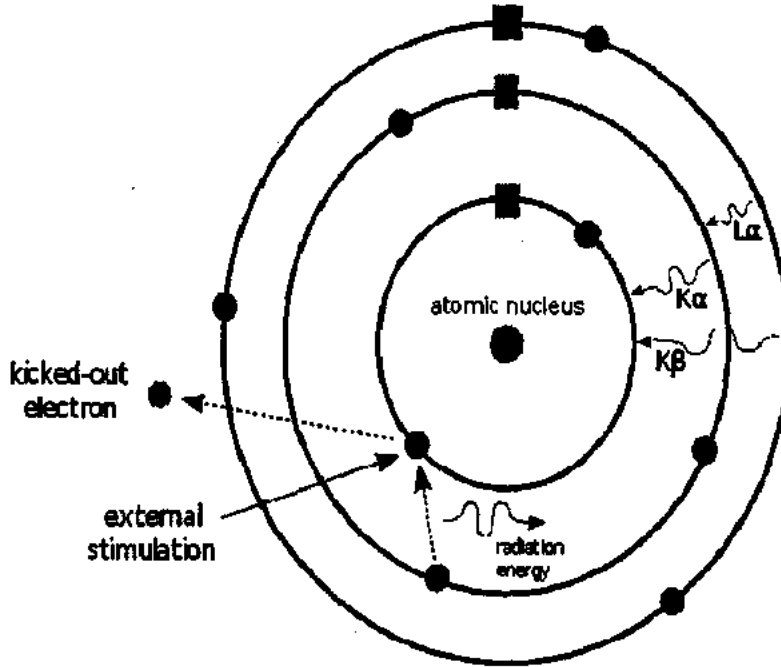


Figure 2.4: Schematic diagram of working principles of EDS [66]

## 2.4 Fourier Transform Infra-red Spectroscopy (FTIR)

It is mostly used for molecular analysis of the sample and is a non-destructive technique. The main feature of FTIR is to characterize solid and liquid samples. This spectroscopy involves the interaction between a material and electromagnetic radiation called infrared and this interaction is the main theme of FTIR spectroscopy. Since the energy of a molecule is equal to the sum of vibrational, rotational, translational and electronic energy levels. Therefore the infrared waves primarily linkage with the molecular vibration. When the IR waves interact with a molecule then it is excite to an upper state by absorbing Infra Red radiation provided its energy matched with the vibrational energy level of the molecule. IR spectroscopy gives fingerprint data on the chemical composition of the material and useful for several types of analyses. FTIR uses Fourier Transform function for digitizes the interferogram and display spectrum therefore it is called FTIR.

FTIR instrument attain wide spectra from NIR to FIR spectra therefore for spectroscopic purpose it is split up into three IR regions; near IR region ( $400-10\text{ cm}^{-1}$ ), mid IR region ( $400-4000\text{ cm}^{-1}$ ), far IR region ( $4000-14000\text{ cm}^{-1}$ ). Here we use mid IR region frequency and divide further into two parts as shown in Figure. Bands are the finger print of each molecule and are found in the region of ( $1300-400\text{ cm}^{-1}$ ); these bands are used only to compare spectra of one compound to another. While the band ( $4000-1300\text{ cm}^{-1}$ ) indicates what type of functional group is attached in this region.

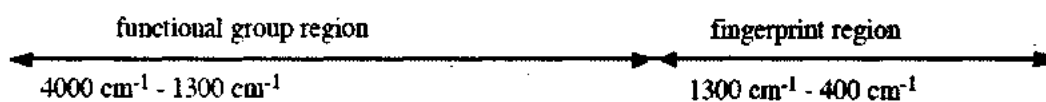


Figure 2.5: Band of functional group and finger print

The most familiar interferometer used in FTIR is a Michelson interferometer. It comprises of two perpendicularly plane mirrors and a beam splitter. In plane mirrors one is fixed and the other is movable while the function of beam splitter is to divide beam into two paths as shown in Figure 2.6 [67]

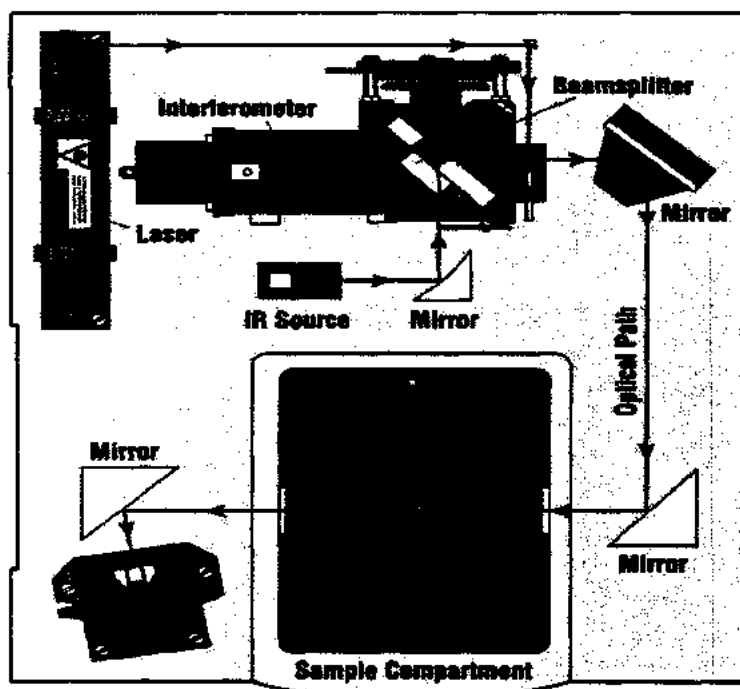


Figure 2.6: Diagram of FTIR set up [67]

### 2.4.1 Procedure

- KBr tablets are mixed with sample in ratio of 2:98 in order to expose hidden and unhidden parameters in the sample and then press for FTIR characterization.
- KBr tablets are used to acquire the background of FTIR spectrum at hundred scans of FTIR spectrometer.

## 2.5 Photoluminescence Spectroscopy (PL)

Luminescence means the emission of light from material but ensuring not by heat. Thus Photoluminescence can be defined as when high energetic photon strike with material, the electron excited from ground state to upper state of an atom, ultimately excited electron relax and comes back to ground state with emitting light called Photoluminescence.

Photoluminescence measurements are non destructive and used generally for the calculation of band gap, impurity levels and recombination mechanism. In the present work we have used the He-Cd source with excitation wavelength 325nm to determine the emission spectra of the samples. A graphical representation of PL setup is shown in Figure 2.7 [68].



Figure 2.7: A graphical representation of PL set up [68]

In PL technique, the light is incident on the sample to excite atoms and as a result the released luminescence is converge with the help of a lens and passes across an optical spectrometer onto a photon detector. The spectral distribution and time dependence of the emission are related to electronic transition probabilities within the sample and provide useful information about structure, impurities, chemical composition, energy transfer and kinetic process.

## 2.6 Raman Spectroscopy

It was discovered by C.V. Raman in 1928 and admitted as a non-destructive technique for chemical analyses. Raman spectroscopy based on inelastic scattering of atoms or molecules by laser when laser light interacts with phonons of the sample. As a result the energy of laser photons being shift up or down and gives information regarding the phonon modes in the sample

The Raman effect occurs within three modes, Rayleigh scattering, stoke Raman scattering and anti stoke Raman scattering as shown in Figure 2.8 [69]. When incident light interacts with a molecule, a phonon in a ground vibrational state is excited to virtual state. It relaxes and then comes back to the same state which means that there is no change in frequency. This is called Rayleigh scattering or elastic scattering. In stoke scattering, phonon initiate with ground state and jump to virtual state. It relaxes to energy state that is higher to its ground state. For anti-stoke scattering, a phonon begins with vibration state that is higher than ground state. It is excited to virtual state then relaxes back to ground vibrational state. Of these two stokes scattering, stoke scattering is used for Raman measurement because most electrons are in ground vibrational state at room temperature.

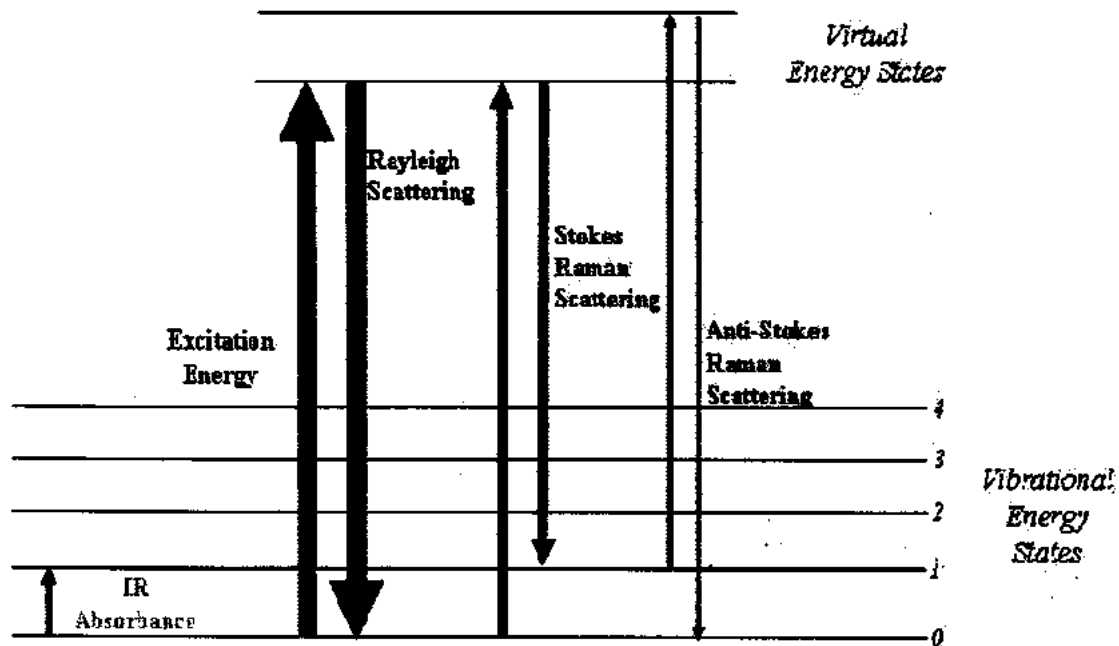


Figure 2.8: Energy level diagram of Raman scattering [69]

Raman spectroscopy is highly sensitive even to smallest difference in geometry, bonding and structure within the molecule. This sensitivity is helpful to examine different allotropes of carbon where atoms are dissimilar in position and nature of bonding to one another. One of the most important applications about Raman measurements is that it requires no sample preparation.

Raman spectrum of graphene reveals an easy structure distinguished by three Raman bands named G, D and 2D bands. They contain key facts regarding thickness and defects of graphene layer attained by evaluating the band shape, band's peak position, and  $I_D/I_G$  ratio. The graphical representation set up of Raman spectroscopy is shown in Figure 2.9 [69].

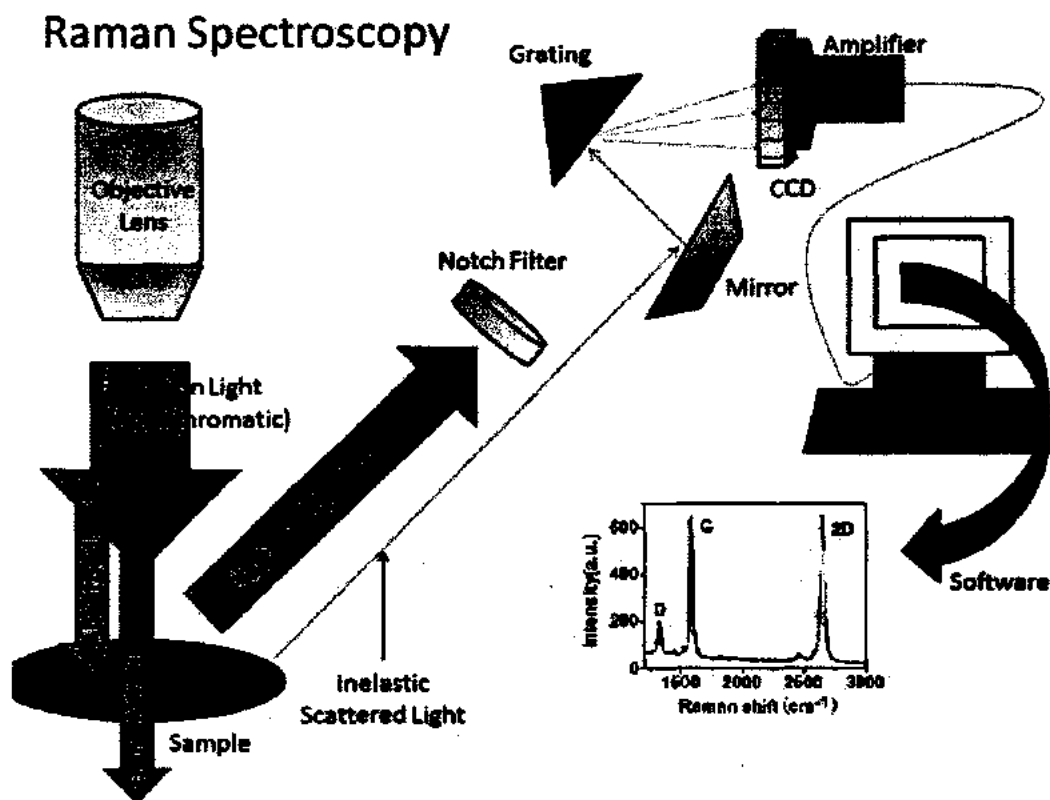


Figure 2.9: Graphical representation of Raman Spectroscopy set-up [69]

## 2.7 Diffusion Reflectance Spectroscopy (DRS)

Diffusion reflection spectroscopy is perfect tool for powder in the range of NIR and mid IR range. DRS give precise and exact value while PL gives estimated values of the optical band gap of nanostructure materials. It saves time instead of mixing powder with non-absorbing material. The sharp spectral lines of atoms or ions have been observed in DRS due to transition between quantum levels. These spectral lines are features of particular atoms or ions and used for fingerprint purpose. Therefore on behalf of DRS other calculations like photon energy and band gap can be determined accurately. In solids, there are large number of atoms or molecules therefore the atomic levels split up into continuous band between conduction and valence band. As a result make their optical spectra broad. The gap between conduction and valence band is assigned as band-gap.

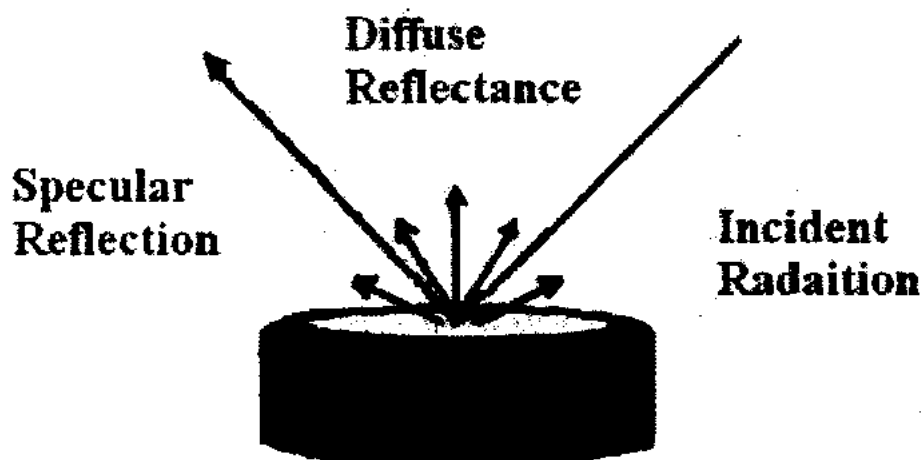


Figure 2.10: The Process of DRS irradiated by light [70]

The Figure shows a process when happening during irradiation of incident beam on a sample. The incident light is scattered, reflected and transmitted through the sample. The diffuse scattered and back reflected light is collected by the accessory and targeted to the detector. The fraction of beam which is scattered in sample is said to be diffusion reflection. The specular reflections sometimes execute changes in band gap. For this purpose we dilute sample with non-absorbing matrix like KBr to minimize these effects.

In DRS, the relation between diffusion reflectance of the sample ( $R\alpha$ ), scattering ( $S$ ) and absorption coefficient ( $K$ ) are related by Schuster-kubelka- Munk (SKM) function and is given

by

$$\frac{k}{s} = \frac{(1-R\alpha)^2}{2R\alpha} \quad (2.4)$$

Where  $R_d$  is the diffusion reflectivity,  $k$  is the absorption coefficient and  $s$  the scattering co-efficient from a layer of sample

The relation  $(\alpha h\nu) = A(h\nu - E_g)^n$  is applicable only when  $\alpha$  is replaced by  $\frac{k}{s}$

Where  $A$  is constant,  $\nu$  is the frequency of light,  $E_g$  is the band gap and  $n$  have values  $\frac{1}{2}$ ,  $\frac{3}{2}$ ,  $2$  and  $3$  depending upon the type of inter band transition that is corresponding to direct allowed, direct forbidden, indirect allowed and indirect forbidden transitions. The absorption wavelengths are measured by converting reflection wavelength using SKM function. The direct band gap and indirect band gap can be measured by drawing Tauc plot between  $F(R)$  and photon energy with their respective  $n=1/2$  and  $n=2$ .

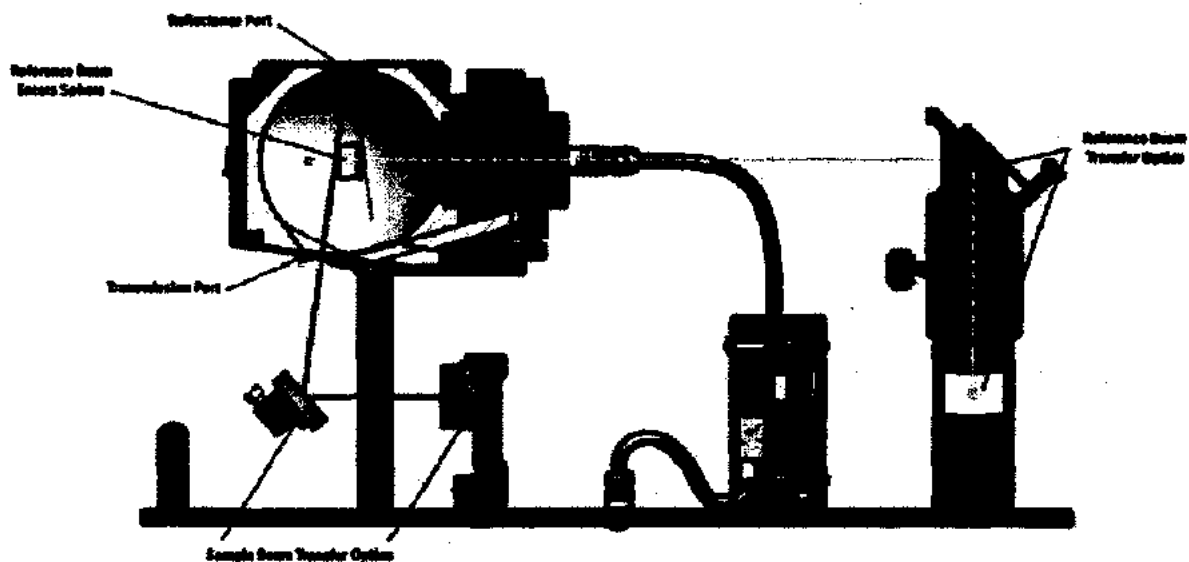


Figure 2.11: Diffusion Reflectance spectroscopy set-up [71]

### 3 Chapter No.3 Synthesis Techniques

This chapter is based on the discussion related to the constituent's materials and about synthesis technique employed during GNP-ZnO nanocomposites preparation and synthesis of ZnO nanostructures.

#### 3.1 Synthesis of graphene-inorganic nanocomposites

The synthesis of graphene-inorganic nanocomposites can be divided into two fundamental groups.

➤ **In situ synthesis method**

➤ **Ex situ synthesis method**

##### 3.1.1 In situ synthesis method

This method concerns the development of nanostructure in the existence of pure graphene or chemically treated graphene sheets and then nanostructure grow straightway into nanomaterials just as nanorods, nanoparticles, nanofilms and nanowires on the GNP sheets surface, which come under the category of in situ techniques.

###### 3.1.1.1 Advantages

The major advantage of in-situ method is to avoid protecting surfactant or extra linker molecules which may involve a deadly laboratory practice, and also affect the purpose of nanocomposites.

One more advantage is that different physical and chemical fabrication methods can be used, like direct decomposition of precursors in solutions, deposition methods, solvothermal or hydrothermal methods, sol-gel processing, gas-phase deposition, and so on.

##### 3.1.2 Ex situ synthesis method

This method includes the earlier fabrication of nanomaterials with own desired size and morphology, then customized and then linked to the pure graphene or functionalized graphene sheets, this is termed as ex situ techniques.

### 3.1.2.1 Advantages

In comparison with in situ method, the superior scattering about, size, and the control of the second ingredient in feeding amount on graphene can be performed using self-assembled techniques.

### 3.1.2.2 Covalent interactions

In this interaction, GO and RGO except from pristine Graphene contain large amount of oxygen include function groups, is to be used for inorganic nanostructures.

### 3.1.2.3 Non-covalent interactions

On the other hand, inorganic nanostructures can be firmly attached to graphene sheet by means of hydrogen bonding, Vander Waals forces, electrostatic interaction or p-p stacking. In non-covalent interaction, electrostatic interactions and p-p stacking have been generally used in the fabrication of graphene-inorganic nanocomposites.

## 3.2 Constituent's Materials

Graphene nanoplatelets (GNPs) of thickness 5-20nm and length with 2 $\mu$ m have been used. These were purchased from Xiamen Knano Graphene Technology Company limited, China. GNPs have more than 99.5% carbon purity. ZnCl<sub>2</sub>, NaOH and acetic acid have been used for synthesis of ZnO nostructures. Ethanol and distilled water has been used as a solvent.

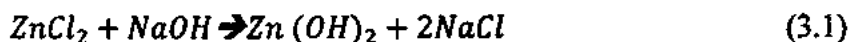
## 3.3 Preparation of ZnO nanostructures

There are different approaches for the fabrication of ZnO nanostructures like sol-gel method, hydrothermal/solvothermal method, co-precipitation method etc. But here we have used co-precipitation method for ZnO NPs due to its simplicity and rapid preparation.

The zinc oxide nanoparticles were fabricated by co-precipitation approach using sodium hydroxide (NaOH) and zinc chloride (ZnCl<sub>2</sub>) just as precursor. Zinc chloride of weight 1.36 g was added to 100 ml of distilled water. Then the zinc chloride solution was kept under steady stirring using temperature based magnetic stirrer with a temperature of 80 °C in order to completely dissolve the zinc chloride and increase the speed of solubility. Similarly sodium

hydroxide of weight 4g was also added to 100ml of distilled water and kept under constant stirring using magnetic stirrer. Now NaOH solution was added to zinc chloride solution with drop by drop action using pipit until the solution attained pH 10. During this process 2ml of acetic acid was also added to zinc chloride solution in order to change zinc chloride into zinc cations. With drop by drop action of NaOH, the color of solution becomes milky which show that precipitations were made in the solution. The solution was granted to dispose and the resilient was carefully abandoned. The resting solution was centrifuged at 10, 000 X RPM for few minutes. The obtained nanoparticles were washed 4 to 5 times by distilled water to clear away byproducts and the excessive starch bound with the nanoparticles. Then the nanoparticles were dried at approximately 80<sup>0</sup>C temperature for overnight. During drying, zinc hydroxide was converted into zinc oxide completely.

The chemical reaction for Zinc hydroxide is given below



After drying Zn (OH)<sub>2</sub> is converted into ZnO and explained by the equation below.



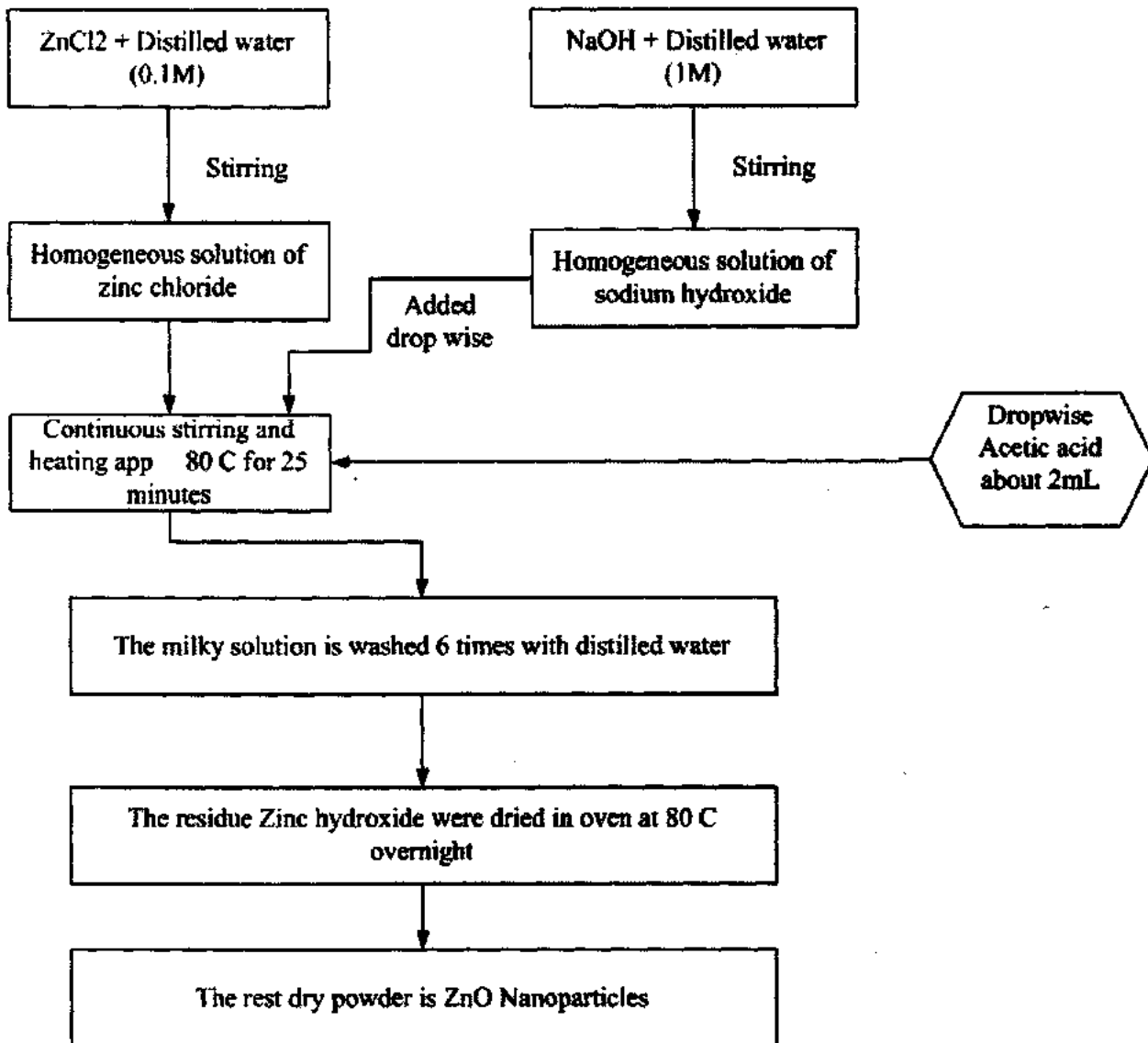


Figure 3.1: Flow chart for Preparation of ZnO nanoparticles

### 3.4 Dispersibility of graphene nano platelets (GNPs)

Graphene nanoplatelets are very thin with relatively large diameters. Like other nanoparticles, Graphene nanoplatelets also raise some issues due to its small size and flat shapes. Due to its flat shape GNPs are very sensitive to weak forces like Vander Waals forces and tends to re-aggregate in dry state. GNPs are dispersive in organic or non-aqueous solvents but mostly non-dispersive in organic solvents. GNPs are hydrophobic in nature and not disperse in aqueous solvents without surfactants or dispersion aids

### 3.5 Uniform dispersion of graphene nano platelets (GNPs)

Pristine graphene nano platelets (GNPs) show poor dispersibility in aqueous medium and form large aggregates with size up to several millimeters. Due to its hydrophobic nature, GNPs faces some limitation in their promising application in the field of composites. For the excellent performance of inorganic GNP composites, a uniform dispersion of GNPs and their strong adhesion with inorganic ZnO NPs are high imperative.

There are several ways for the proper and effective dispersion of GNPs into composites. Use of shear force via sonic waves is easiest method to de-agglomerate GNPs. Secondly dispersion aids can be used for good dispersibility especially in polymers.

#### 3.5.1 Ultrasonication

It is important to note that GNPs dispersion depends on the size of nanoplatelets, the medium and the energy used for dispersion and the time allowed. The uses of surfactants improve the stability of suspension of particles.

GNPs can be dispersed in aqueous solution using several ways; the simplest method to de-agglomerate the GNPs is the use of sonic waves. This process is called ultra-sonication. The ease of this process gives rapid result in the form of GNPs dispersion; however, this causes the adverse effects on morphology of GNPs. The ultrasonication process for the longer period with high intensity can reduce the length of GNPs.

The optimized use of sonication process is acceptable for GNPs. The other effective procedures employed to enhance the dispersibility of GNPs are the attachment of chemical groups on the surface of GNPs called functionalization.

### 3.6 Development of nanocomposites

Uniform dispersibility of GNPs into nanocomposites play very important role for the fabrication of GNPs-ZnO nanocomposites. In order to achieve this goal, the ex-situ method was used to fabricate the GNP-ZnO nanocomposites.

**3.7 Fabrication Process of GNPs-ZnO nanocomposites**

The fabrication of GNP-ZnO composites has been followed by ex-situ method and the following step by step procedure has been adopted for its fabrication.

- i. In the start, 50 mg GNPs have been used to disperse in 250 ml ethanol under the sonication process for one hour and covered beaker with aluminum sheet.
- ii. After one hour, 500mg ZnO NPs have been added and sonicated further for one hour.
- iii. In last step, the contents were transferred to a clean beaker and heated in a furnace at 200<sup>0</sup>C for 2 hours. The final powder is designated as 10 wt % GNP-ZnO

we have prepared different samples with varying weight percent of GNPs with respect to ZnO fixed weight percent. The process was repeated with varying mass of graphene nanoplatelets, viz. 75 mg, 100mg, 125mg and 150 mg and the final products were designated as 15 wt % GNP-ZnO, 20 wt % GNP-ZnO , 25 wt % GNP-ZnO and 30 wt % GNP-ZnO respectively. Graphical representation and flow chart for the formation of 10 wt % GNP-ZnO nanocomposites have shown in Figure 3.2(a) and (b) [72].

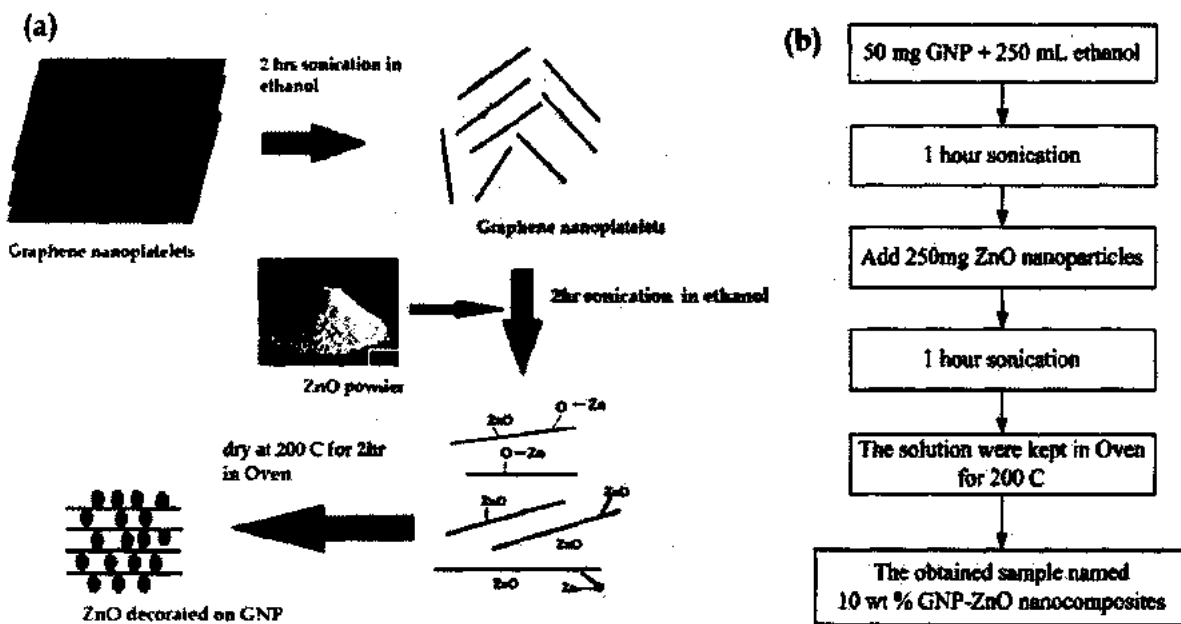


Figure 3.2: (a) Graphical representation of the formation of Graphene Nanoplatelets decorated with ZnO nanoparticles (b) Flow chart for 10 wt % GNP-ZnO nanocomposites [72]

### 1.1 Preparation of Agar diffusion assay for Antibacterial Test

Agar disc method was employed to study the antibacterial property with our prepared nanostructures. The bacterial suspensions (35mg/ml) were prepared and then it was inoculated onto the whole surface of agar plate with a sterile cotton-tipped swab. The disks with 5 mm in diameter impregnated with the prepared samples and were placed on the surface of agar plate using a sterile pair of forceps. These agar plates were growth at 37°C for 24 hrs and zone of inhibitions were calculated in millimeters (mm) with the help of a ruler or scale as shown in Figure 3.3 [73].

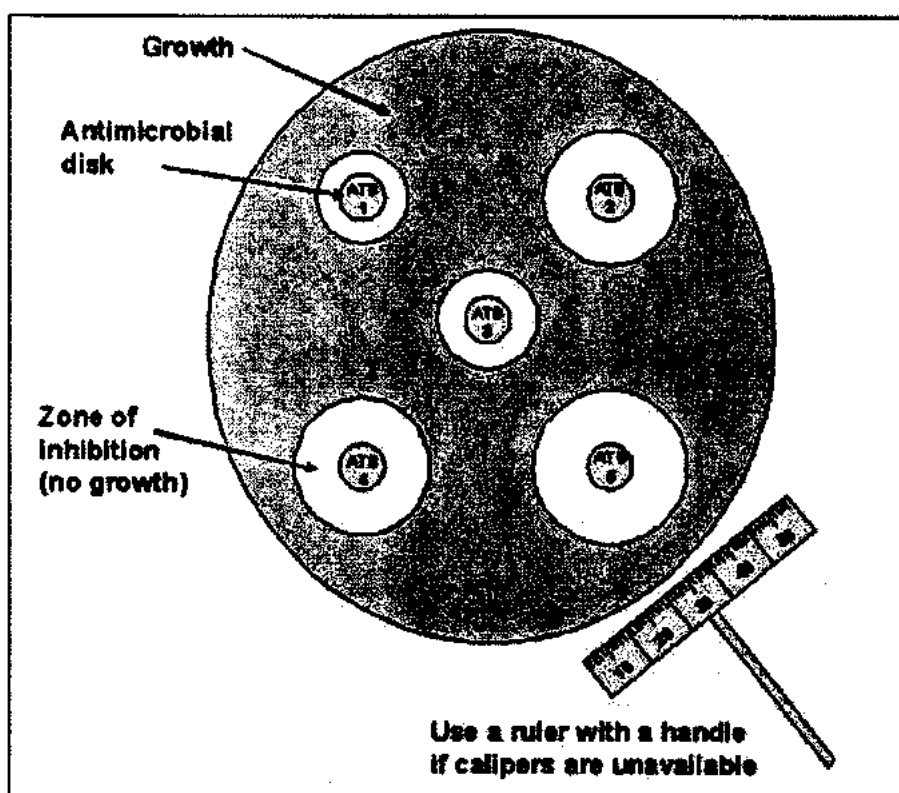


Figure 3.3: Agar plate with disk surrounded by zone of inhibition [73]

## 4 Chapter No.4 Results & Discussions

The prepared Graphene Nanoplatelet-ZnO nanocomposites were characterized by SEM, X-ray Diffraction, EDX, Raman Spectroscopy, FTIR and PL.

### 4.1 X-ray Diffraction Analysis:

In the XRD pattern of pure GNP as shown in Figure 4.1, there are three broad bands at angles ( $2\theta$ )  $26.5^\circ$ ,  $42.4^\circ$ ,  $43.9^\circ$ ,  $54.6^\circ$  and  $77.4^\circ$  corresponding to (002), (100), (101), (004) and (110) planes of graphite respectively which were in good agreement with hexagonal structure of carbon JCPDS Card No.75-1621. While the planes (100) and (101) regarding to  $42.4^\circ$ ,  $43.9^\circ$  are mixed with each other showing little hump in GNPs pattern. It may be due to little bit strain between two angles which are not differentiated. The average crystallite size of GNPs as determined by Debye Scherer formula is about 26.5 nm

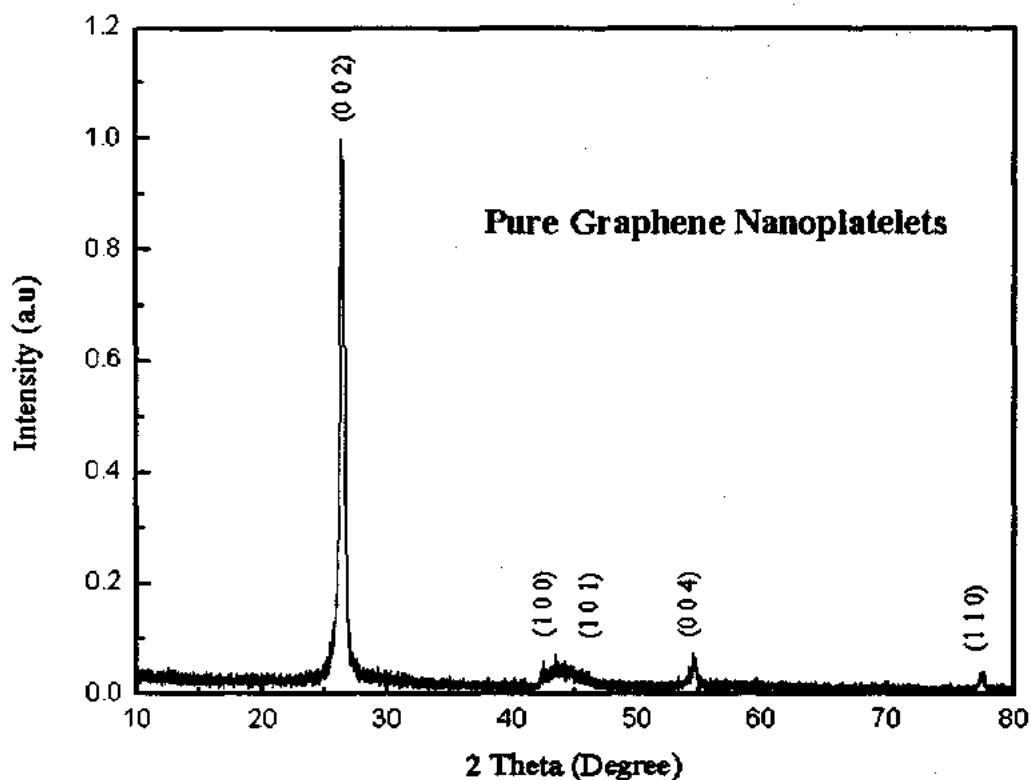


Figure 4.1: XRD pattern of pristine GNPs

The XRD diagram of ZnO nanoparticles is displayed in Figure 4.2 and it reveals that all the diffraction peaks of ZnO nanoparticles are consistent to hexagonal wurtzite structure of ZnO which are in good agreement with the JCPDS Card 36-1451. There are eight main diffraction peaks located at angles ( $2\theta$ ) of  $32.12^\circ$ ,  $34.77^\circ$ ,  $36.54^\circ$ ,  $47.94^\circ$ ,  $56.85^\circ$ ,  $63.09^\circ$ ,  $68.21^\circ$  and  $69.37^\circ$  corresponding to (100), (002), (101), (102), (110), (103), (200) and (201) crystal facet correspondingly. The average crystallite size of the ZnO nanoparticles as calculated using Scherer formula was  $\sim 30.6$  nm. It is clear from calculation that the ZnO nanoparticles has a hexagonal phase with lattice constants  $a = 3.2492 \text{ \AA}$ ,  $c = 5.20661 \text{ \AA}$ .

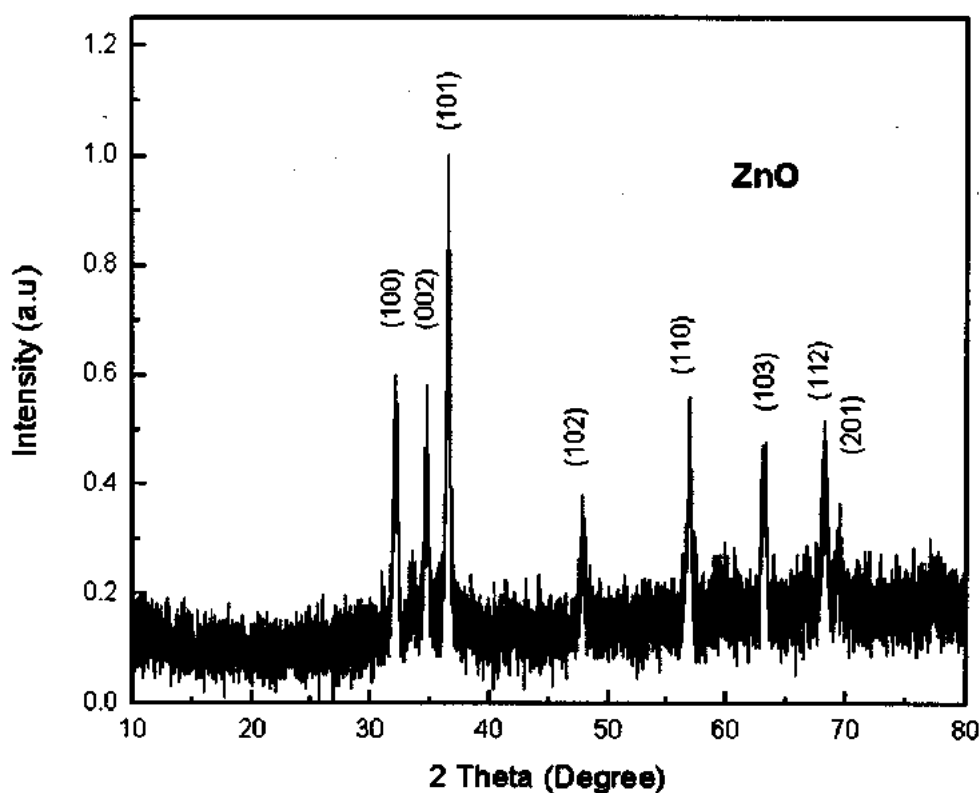


Figure 4.2: XRD pattern of pristine ZnO sample

It is clearly obvious from Figure 4.3 that the XRD patterns of GNP-ZnO nanocomposites reveal the formation of hexagonal wurtzite crystal structure. It is observed that as the loading of GNP is increased, the intensity of the peaks corresponding to ZnO phase in the composite also increases as compared to pure ZnO, which shows not only that samples have been made but also confirm the crystallinity of the GNP-ZnO composites has been improved as well. The plane

(002) which appeared at angle  $26.5^{\circ}$  corresponds to GNP and very weak in the XRD pattern of GNP-ZnO composites as compared to pure GNP. This indicates that ZnO nanoparticles are anchored well on the graphene nanoplatelets surface. The absence of others GNP peak in GNP-ZnO composites was due to the higher concentration of the ZnO precursor and suppressed in the GNP-ZnO composites and therefore, the GNPs surface may be well covered by ZnO. The absence of other peaks except ZnO and GNP revealed the quality of the prepared samples.

The weak diffraction peak for GNP in the 10 wt % GNP-ZnO composite reflects the fine GNPs dispersion across ZnO nanoparticles and also due to low amount of GNP loading in the composite. Moreover, it has been observed that with increase in weight percent loading of GNPs on ZnO, the intensity of diffraction peak for GNP at angle  $26.5^{\circ}$  is also increasing but at 30 wt % GNP-ZnO composite, the intensity decreases which may be due to ZnO nanoparticles are well dispersed on GNPs. The loading of GNPs on to the ZnO nanoparticles does not change peak positions corresponding to GNPs and ZnO, representing no main change in the crystal structures of these constituents. The lattice constants "a" and "c" were calculated for (100) (002) and (101) planes of ZnO in composites using the following equation

$$a = (\lambda/\sqrt{3}, \sin\theta) \quad \text{and} \quad c = \lambda/\sin\theta \quad (4.1)$$

The lattice constants "a" and "c" are found to be same as for pure ZnO NPs which means that on loading of GNPs, there is no change in the crystal structure of ZnO.

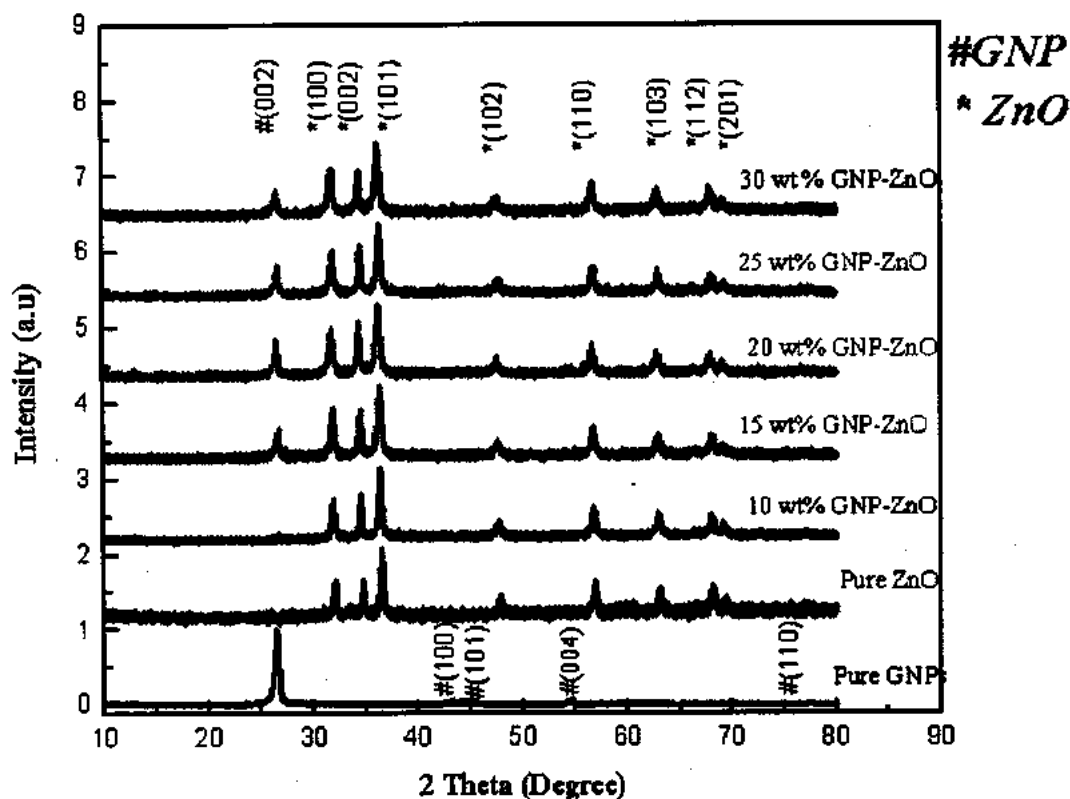


Figure 4.3: XRD patterns of pure GNP, pure ZnO NPs, 10wt% GNP-ZnO, 15wt% GNP-ZnO, 20wt% GNP-ZnO, 25wt% GNP-ZnO, 30wt% GNP-ZnO nanocomposites

## 4.2 Morphology of GNP-ZnO nanocomposites

Morphology plays an essential role in nano science since it shows different physical and chemical properties of composites. Therefore it is necessary to understand morphology of GNPs and GNP-ZnO nanocomposites. The morphological characterizations have been performed using FESEM from Figure 4.4 (b), (c) and (d), it can be observed that the FESEM images of GNP-ZnO nanocomposites at different weight percent loading of GNP shows nearly same morphological features. As discussed in introduction of this thesis that GNPs act as a sheet or platelet for decorating different size of ZnO nanoparticles and the platelet acts as a bridge between different ZnO nanoparticles. As can be seen in GNP-ZnO composites that ZnO nanoparticles are strictly stick to the surface and edges of GNPs. In Figure 4.4(b), the sample with 10% weight loading of GNPs on ZnO nanoparticles, the ZnO nanoparticles which are agglomerated have spherical shapes and their average size is in ranges from 100 to 150 nm. These nanoparticles are

agglomerated with each other to make big nanoparticles. It is also clear from FESEM images that no individual ZnO nanoparticles can be seen separately. It must be clear that the size of ZnO nanoparticles in FESEM may be due to agglomeration of ZnO nanoparticles and depend on the preparation of ZnO. It is also observed a minute part of a GNP in composites where majority area of GNP is covered by ZnO nanoparticles as shown in Fig 4.4 (c) and (d). In Figure 4.4(a) i.e. in morphology of pure GNPs, GNPs aggregate with an average size of few microns, well distributed and adjacent to each other, implying the formation of a continuous network and also in GNP-ZnO composites on which ZnO nanoparticles are anchored on GNPs surface and its edges.

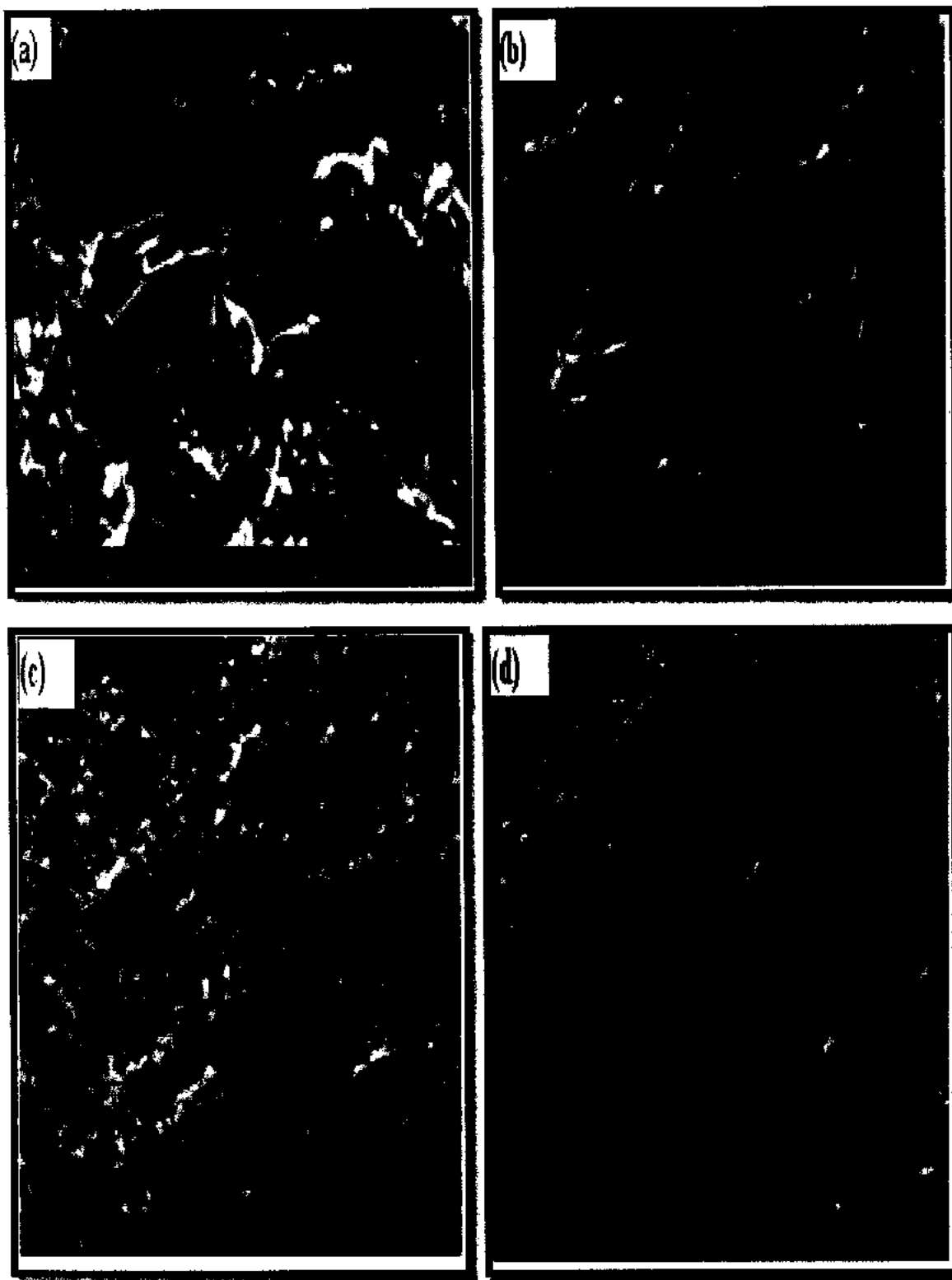
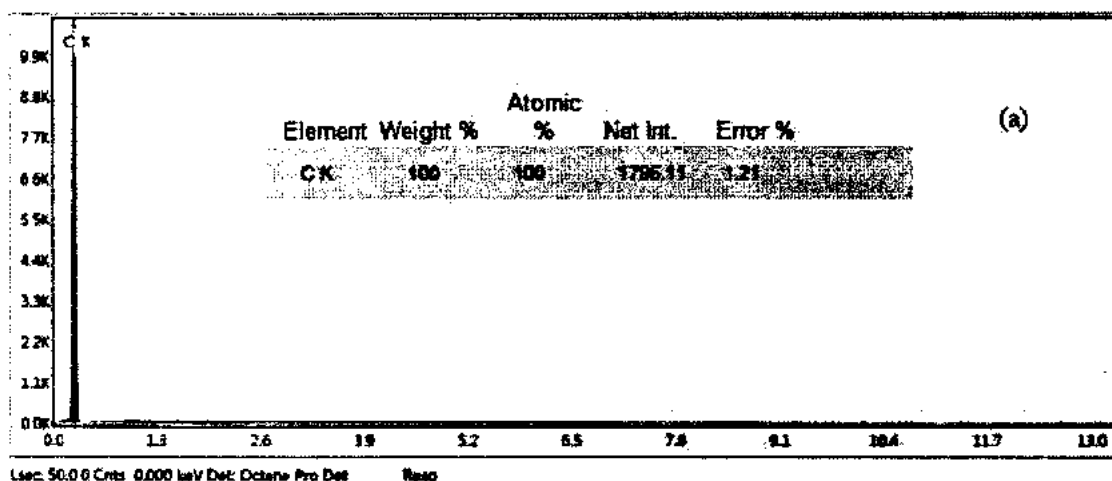


Figure 4.4: FESEM layout of (a) GNPs (b) 10wt% (c) 20wt% (d) 30wt% GNP-ZnO nanocomposites

### 4.3 EDX of GNPs and GNP-ZnO nanocomposites

The quantitative analyses of pure GNPs and composites were investigated to EDX analysis in order to validate the chemical compositions of the composites. The EDX spectra of pure GNP and different weight percent GNP-ZnO composites have shown in Figure. 4.5 (a), (b), (c) and (d). It is very obvious from Figure. 4.5(a) that only carbon element strong peak was found in the spectrum as our GNPs composed of 100% pure carbon and there was no impurity found in the GNPs sample. Similarly the composite samples synthesized by ex-situ method are free from elemental impurities and these consists of Zn, O, and C. Figure 4.5(b), (c) and (d) clearly show that atomic percentage of carbon increases alternately which validate different weight percent of loading GNP on ZnO in composite. It also reveals that Zn intensity is greater in FESEM images which shows greater amount of ZnO. In Figure 4.5 (d) some extra peaks are found in spectra which were of elements Chlorine (Cl) and Aluminum (Al). Aluminum may be due to holder where samples have been kept for characterization of FESEM because no such impurities found in the same sample in characterization of XRD and Raman while Chlorine impurities may be developed during synthesis of this sample.



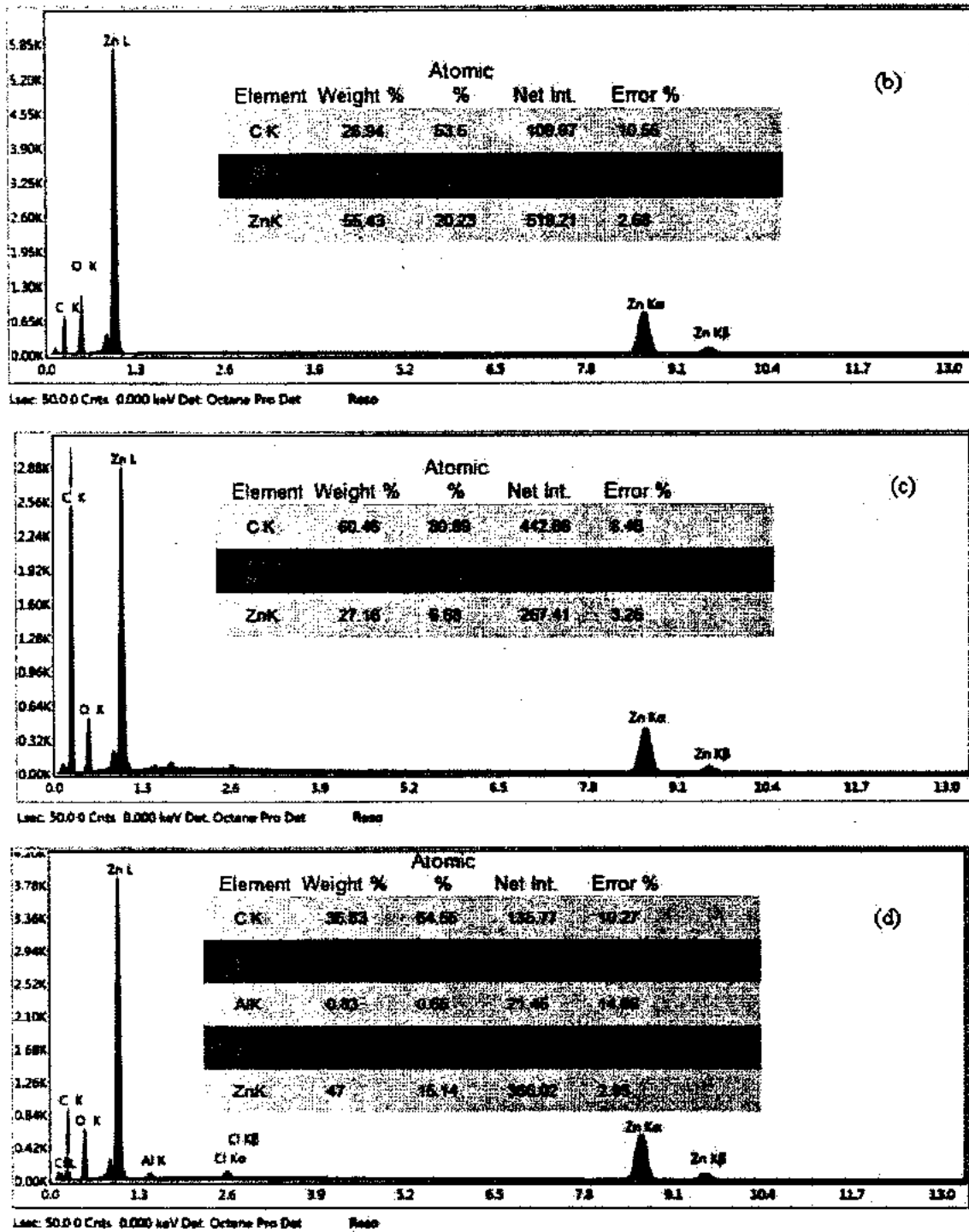


Figure 4.5: EDX spectra of (a) GNP (b) 10 wt % GNP-ZnO (c) 20 wt % GNP-ZnO (d) 30 wt % GNP-ZnO nanocomposites

#### 4.4 Vibrational study of GNPs-ZnO nanocomposites

Raman spectroscopy is most sensitive tool to differentiate carbon based nanostructures [74]. The Raman spectroscopy for GNPs and GNP-ZnO nanocomposites measured at room temperature. Figure 4.6 reveals the crystallization of hexagonal ZnO in different weight percent of GNP composites are in good accomplishment with XRD results. The Raman spectrum of GNPs have revealed three broad peaks at  $1366\text{ cm}^{-1}$  and  $1594\text{ cm}^{-1}$  and  $2735\text{ cm}^{-1}$  corresponding to D, G and 2D band. The D band corresponding to the breathing mode of k-points phonons of  $A_{1g}$  symmetry and G bands assigned to the  $E_{2g}$  mode phonon of  $sp^2$  carbon atoms, respectively [75]. Figure 4.6 also show the Raman spectra of different weight percent composites, respectively. The Raman spectra of GNP-ZnO composites displayed the modes of ZnO. The ZnO nanoparticles in the composite shows the standard Raman mode and they are observed at  $438\text{ cm}^{-1}$  ( $E_2$  (high)), [76] defect peak (D-band), and high intense G band and 2D band. As the loading of GNPs with different weight percent is increased in GNP-ZnO samples, the intensity of  $E_2$  (high) mode decreased as well. The GNPs incorporation suppressing the most ZnO vibration mode peaks. The D-band and G-band have shown blue shift by  $8\text{ cm}^{-1}$  in GNP-ZnO composites depicting that most of the graphene sheets are under strain, due to the interactions with the ZnO particles while the  $I_D/I_G$  ratio (defect ratio) increases from GZ-10% to GZ-30%. Hence, the formation of GNP-ZnO nano-composites confirmed by the micro-Raman analysis and results are corresponding well with XRD results.

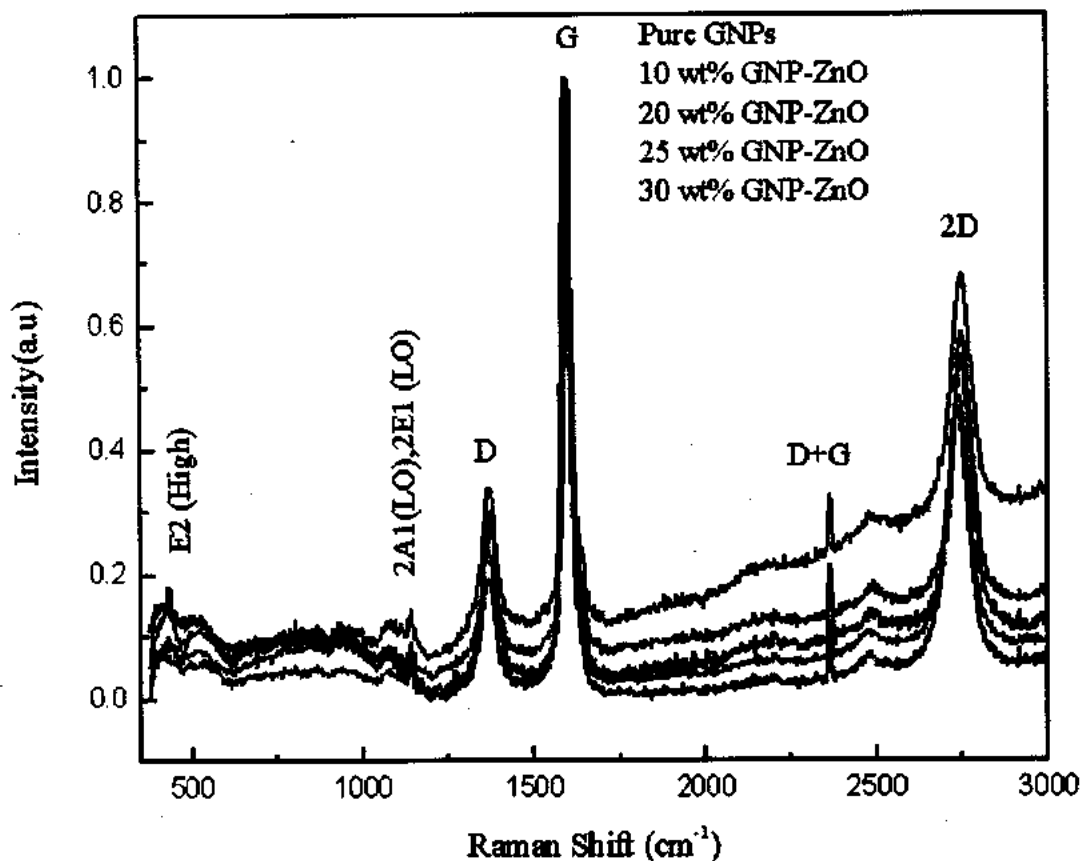


Figure 4.6: Raman spectra of (a) GNPs (b) 10 wt % GNP-ZnO (c) 20 wt % GNP-ZnO (d) 30 wt % GNP-ZnO nanocomposites

#### 4.5 FTIR Analyses of GNP-ZnO nanocomposites

The FTIR spectra of GNP-ZnO nano-composites have been carried out at room temperature. The Figure 4.7 displays infra red spectra ranging in  $450\text{--}4000\text{cm}^{-1}$  which cover the ranges of both ZnO and carbon structure (GNPs). The peaks in GNP-ZnO nanocomposites at  $3417\text{ cm}^{-1}$  indicate the existence of OH groups, and are payable to the existence of moisture in the samples. The peak at  $1642\text{ cm}^{-1}$  can be designated to in plane C=C band and confirms the oscillations of un-oxidized GNPs domains [77]. The functional groups containing oxygen link to GNP-ZnO composites are reported by the bands at  $1410\text{ cm}^{-1}$  and  $1045\text{ cm}^{-1}$ , which resemble to C- OH stretching and C- O stretching vibrations [78]. In GNP-ZnO composite the peak at  $465\text{ cm}^{-1}$  is the feature peak of the Zn-O stretching vibration of ZnO. [79-80]. These in formations certify that the GNP-ZnO nanocomposites have been well prepared.

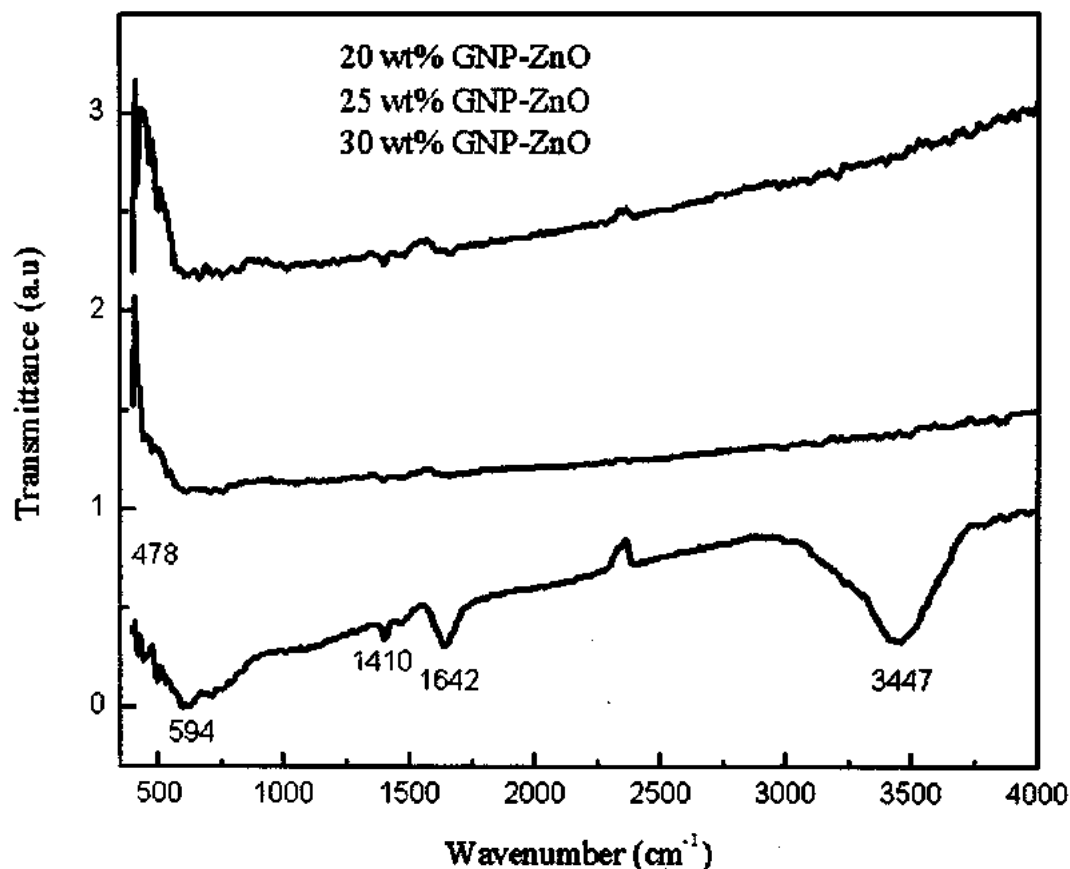


Figure 4.7: FTIR spectra of (a) 20 wt % GNP-ZnO (b) 25 wt% GNP-ZnO (c) 30 wt % GNP-ZnO nanocomposites

#### 4.6 Optical properties of GNPs and GZ nanocomposites

The UV-visible absorption spectra of ZnO and GNP-ZnO composites have shown in Figure 4.8. The keen and sharp absorption peak at wavelength 370 nm indicates the presence of pure ZnO NPs corresponding to band gap of 3.35eV [81] as compared to the reported values of band gap energy of bulk ZnO ( $E_g = 3.37$  eV). It is also observed that GNPs show featureless spectra while the GNP-ZnO composites show absorption spectra in the visible light region. This absorption spectra increase with loading of GNP that is, red-shiftiness of absorption edge occurs as compared to pure ZnO absorption spectra. The maximum absorption of visible light is reported for all GNP-ZnO composites with respect to increase in loading of GNP on ZnO but minimum absorption spectra at wavelength 374 nm is observed for 10 wt %GNP-ZnO composite which is due to low amount of GNP loading. Therefore it is clear that increase in absorption

spectra may be due to involvement of carbon structure in ZnO. This increase in absorption spectra of GNP-ZnO composites towards red-shift may be due to increase of surface electric charges of the oxides and may be due to variation of electron-hole pair creation during irradiation process [82]. It reveals that with the introduction of carbon on ZnO increases the absorption of visible light which is valuable for photo catalytic. The DRS spectra of the ZnO and GNP-ZnO composites displayed strong UV emission band having emission values at ~ 370 nm (3.35 eV), ~ 425 nm (2.91eV), ~452nm (2.74eV), 538 nm (2.3eV) , 553nm (2.24eV) and 597nm(2.07eV) for ZnO, 10wt % GNP-ZnO, 15wt % GNP-ZnO , 20wt % GNP-ZnO , 25wt % GNP-ZnO and 30wt % GNP-ZnO respectively. The band gap was calculated using equation

$$E = \frac{hc}{\lambda} \quad (4.2)$$

Where

$h$ =plank's constt,  $c$ =velocity of light and  $\lambda$ =wavelength of light.

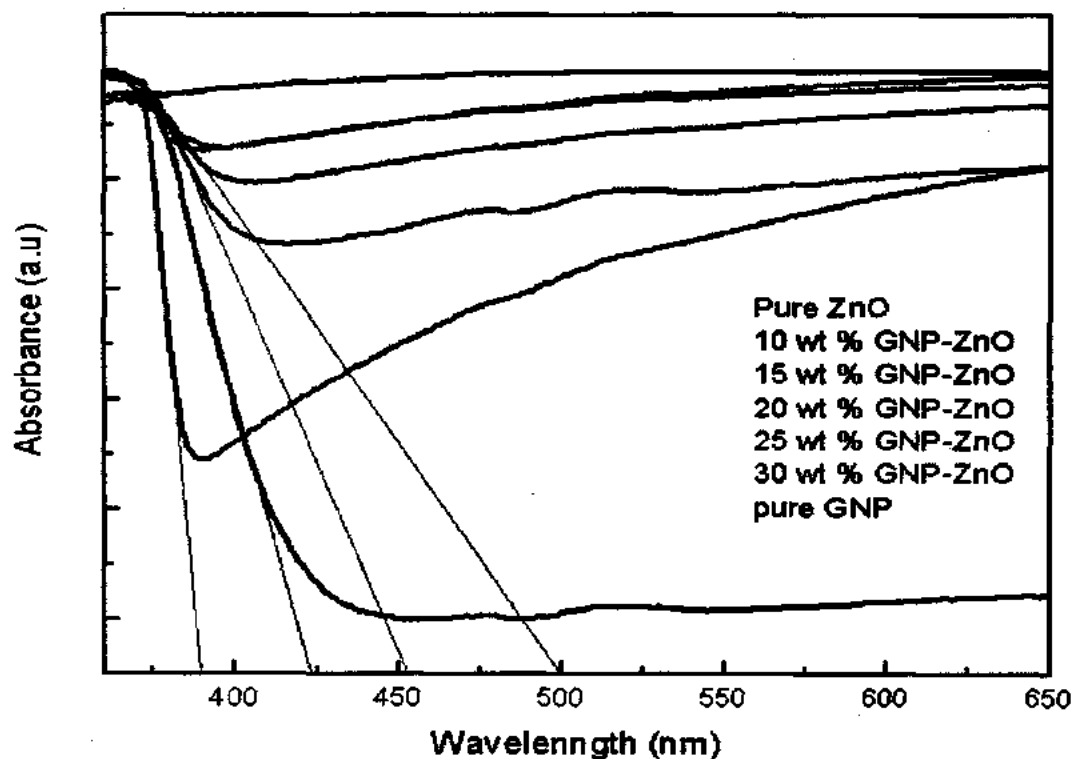


Figure 4.8: DRS spectra of (a) Pure ZnO (b) 10wt% GNP-ZnO (c) 15wt%GNP-ZnO (d) 20wt%GNP-ZnO (e) 25wt%GNP-ZnO (f) 30wt%GNP-ZnO (g) Pure GNP

#### 4.7 Photoluminescence (PL) of GNPs and GNP-ZnO nanocomposites

The PL emission spectra of ZnO and GNP-ZnO composite have been measured at room temperature in the range of 350 - 700nm as shown in Figure 4.9. The excitation source with 325nm of He-Cd (helium-Cadmium) lamp was used for PL spectrum of the GNP-ZnO samples. In the PL spectrum of pure ZnO NPs, one blue emission peak with 410nm observed which appear due to recombination of free excitons [83] As compared to pure ZnO NPs, the same phenomena also observed in the GNP-ZnO composites. In the PL spectra of GNP-ZnO composites, the spectra observed blue shifted in comparison with ZnO and the enhancement increases with the increase of GNPs in composites. Like CNT-ZnO composite, the quenching affects also observed in the PL spectra of GNP-ZnO composites. As it is admitted that like inorganic nanomaterials, ZnO is also good electron donor and graphene is a good electron acceptor. Therefore the PL quenching effect can be described as the electron transfer from conduction band of ZnO to graphene reduces the recombination of electron hole pair and assists to increase charge carrier separation [84, 85]. Thus with the introduction of GNPs into ZnO based composites, the PL intensity decreases. In Figure 4.9 the PL spectrum of ZnO is highest which shows high recombination of electrons and holes. Similarly on different weight percent loading of GNP indicates the lower recombination rate of electrons holes pair under light irradiation as a result emission intensity is decreased. Therefore GNP-ZnO composites increase the photo catalytic potential and. show better photo catalytic action than bare ZnO [86].

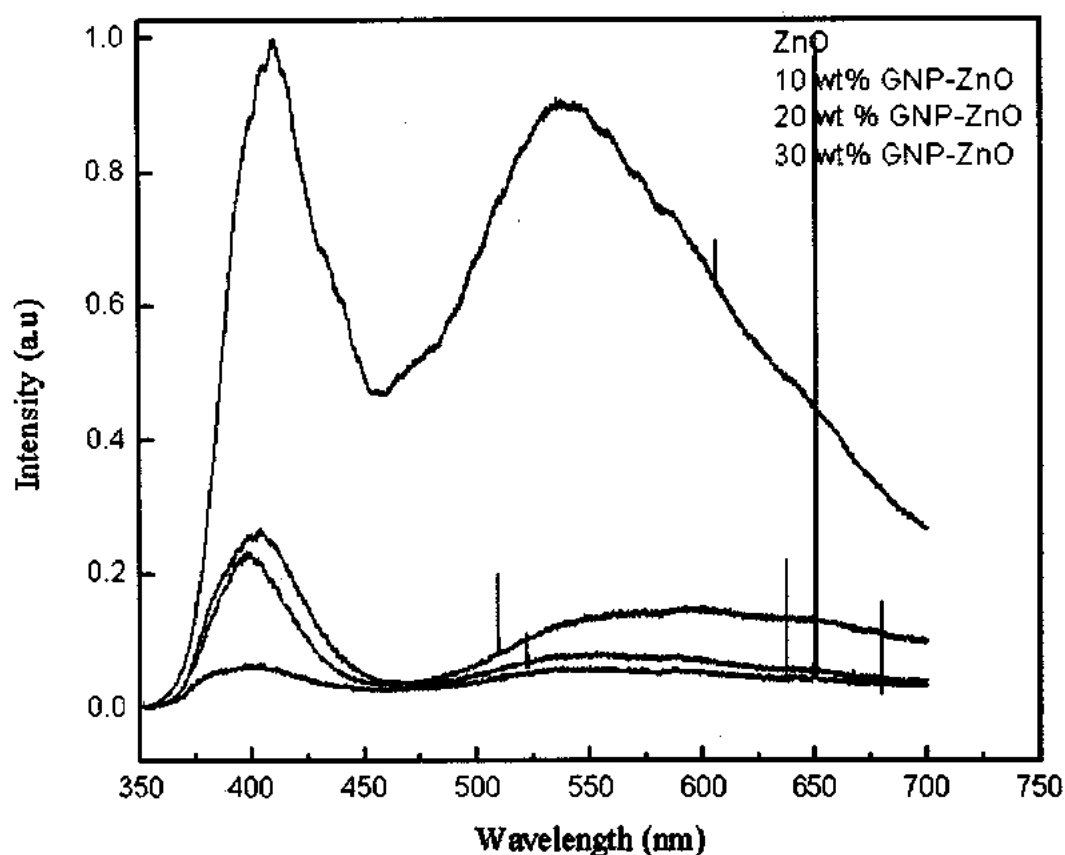


Figure 4.9: PL spectra of (a) Pure ZnO (b) 10wt%GNP-ZnO (c) 20wt%GNP-ZnO (d) 30wt%GNP-ZnO nanocomposites

#### 4.8 Biocompatibility of GNP-ZnO nanocomposites

It can be seen that both ZnO-NPs and GNP-ZnO nanocomposite samples found to exhibit significant inhibitory effect against *E. coli* and *MRSA* bacteria. The diameter zone of inhibition (ZOI) for studied samples were measured and drawn in bar graph in Figure 4.10. The obtained results reveal that the GNP-ZnO nanocomposites show larger inhibition zone against *E. coli* as compared to pure ZnO-NPs. The existence of zone of inhibition suggests that the GNP-ZnO composites have killed more effectively the bacteria than ZnO by direct contact through disruption of bacterial membrane function. It showed that the antibacterial activities of GNP-ZnO composites samples are more effective against *E. coli* bacteria. This may be from the thinner thickness of the peptidoglycan layer of Gram-negative *E. coli* bacteria [87].

In case of *MRSA*, the antibacterial activities of pure ZnO nanoparticles are stronger as compared to GNP-ZnO composites. The cytotoxicity of pure ZnO nanoparticles and composites are linked with several factors such as particle shape and size, release of  $Zn^{+2}$  ions and ROS generation [88]. In GNP-ZnO composites, it is noted that 10 and 15 wt % GNP-ZnO composites have shown decrease in antibacterial activity. In contrast, 20 and 25 wt % GNP-ZnO have shown increase in antibacterial activity as compared to pure ZnO NPs. This result can be explained as follow that a large number of ZnO NPs existed in the small wt % of GNPs and can be attributed to efficient separation of photo-generated electron-hole pairs. Since GNPs could be used as an efficient electron acceptor and transporter [89], suggesting decrease in the antibacterial activity due to decrease in defects of composites. A further loading of GNPs have found to be ineffective in suppressing exciton recombination which could lead to a shield of the active sites of GNPs and also because of the large distance between GNPs and ZnO NPs [90]. Thus ZnO NPs produce more ROS by photo generated electron hole pair on the surface of nanostructure and cause more toxicity in order to death the micro-organism.

These results suggest that the GNP-ZnO composites have a good antibacterial activity against gram negative and gram positive micro-organisms. This anti bacterial activity may be either physical interaction of graphene with the bacteria or oxidative stress of the cell membrane that damage the components of the cell membrane analogous to action of carbon nanotubes.

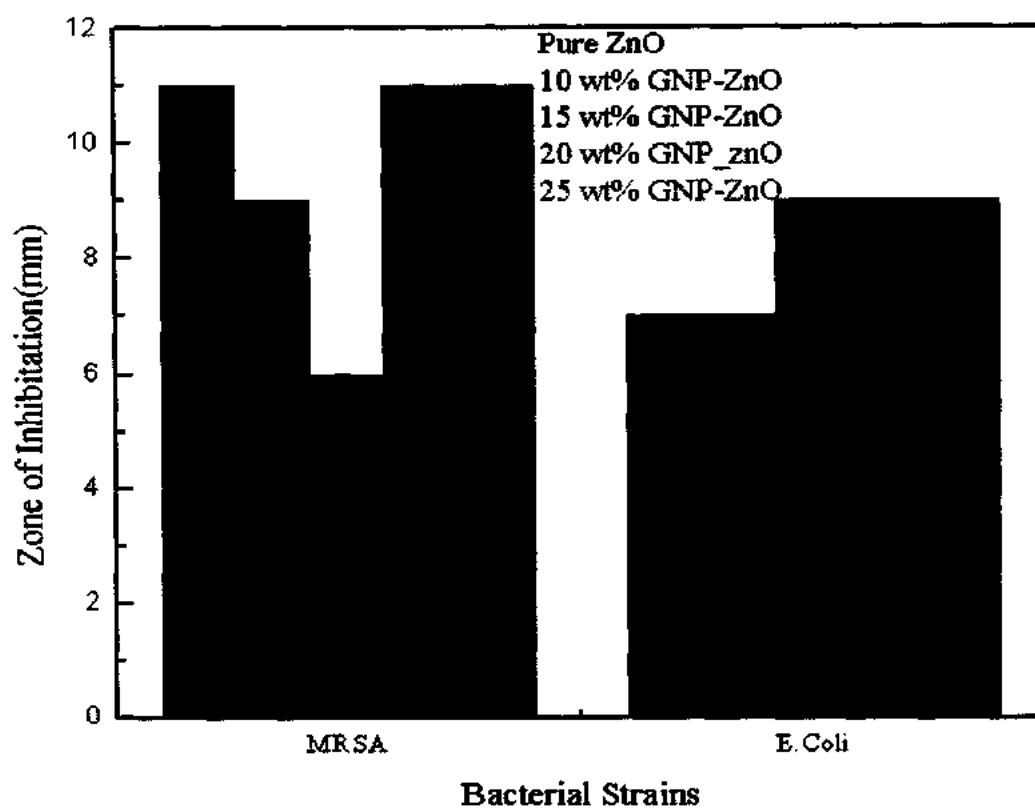


Figure 4.10: Anti-bacterial activity of ZnO and GNP-ZnO nano-composites against MRSA and E.Coli bacteria

### 5 Conclusions:

The GNP-ZnO nanocomposites prepared by ex-situ method. The different weight percent of GNPs loading on ZnO NPs investigated using Raman, XRD, SEM, FTIR, DRS, PL and EDX. As a result the following conclusions have achieved.

- X-ray diffraction pattern of GNP-ZnO nanocomposites revealed that wurtzite structure of ZnO and GNP have anchored well. The peaks intensity of ZnO in composites has found to be increase as compared to pure ZnO which also revealed the confirmation of GNP-ZnO nanocomposites.
- FESEM micrographs of GNP-ZnO nanocomposites have shown that ZnO NPs are well uniformity distributed on GNPs surface and ZnO nanoparticles have agglomerated.
- EDX confirmed the existence of Carbon, Zinc and Oxygen elements. The substantial peaks of Zn created in the spectrum as the weight ratio of this element was very high as compared to carbon.
- The Raman active modes of ZnO nanoparticles  $438\text{ cm}^{-1}$  ( $E_2$  high), confirmed the wurtzite structure and also verified D, G and 2D bands of GNPs in GNP-ZnO nanocomposites.
- The DRS spectra of the ZnO and GNP-ZnO composites have displayed strong UV emission band having emission values at  $\sim 370\text{ nm}$  (3.35 eV),  $\sim 374\text{ nm}$  (3.31eV)  $\sim 538\text{ nm}$  (2.3eV) and  $597\text{nm}$ (2.07eV)respectively.
- The photoluminescence spectra showed that the PL intensity has decreased with the GNPs loading on ZnO as compared to pure ZnO and blue shifted has observed in composites spectrum.
- FTIR results have displayed that ZnO nanoparticles and GNP are attached with each other by functional groups.
- The antibacterial property of GNP-ZnO composites shows that GNP-ZnO composites have killed bacteria more effectively than ZnO due to addition of GNPs which reveals that GNP-ZnO composites are more effective against gram negative than gram positive bacteria.

## 6 References

- [1] Hand book "An Introduction to Metal matrices composites" T.W.Clyne, P.J Withers, University of Cambridge, Feb (1995).
- [2] Hand Book "Ceramic matrce composites" 2<sup>nd</sup> edition by K .K. Chawla.
- [3] K. Upadhya, pp-15-18, May (1992)..
- [4] Horrocks AR, Price D, Fire retardant materials, Woodhead Publishing ISBN 1 85573 4192
- [5] "Carbon matrix composites",by Krashan K. Chawla.
- [6] Ratna D Epoxy Composites: Impact Resistance and Flame Retardancy Rapra Review Reports Volume 16, Number 5, (2005}
- [7] "Graphene based composites" Xiao Huang, Xiaoying Qi, Freedy Boey and hua Zhang.
- [8] Song Bai and Xiaoping Shen" Graphene–inorganic nanocomposites" RSC Advances, Volume 2, 64–98, (2012),.
- [9] N. Li, Z. Y. Wang, K. K. Zhao, Z. J. Shi, S. K. Xu and Z. N. Gu, J. Nanosci. Nanotechnol, Volume 10, 6748–6751, (2010),
- [10] B. J. Jiang, C. G. Tian, W. Zhou, J. Q. Wang, Y. Xie, Q. J. Pan, Z. Y. Ren, Y. Z. Dong, D. Fu, J. L. Han and H. G. Fu, Chem.–Eur.J., Volume 17, 8379–8387 (2011).
- [11] M. Pumera, Energy Environ. Sci, Volume 4, 668–674 (2011).
- [12] S. J. Guo and S. J. Dong, Chem. Soc. Rev, Volume 40, 2644–2672 (2011).
- [13] Y. H. Hu, H. Wang and B. Hu, ChemSusChem, Volume 3, 782–796 (2010).
- [14] Y. G. Zhou, J. J. Chen, F. B. Wang, Z. H. Sheng and X. H. Xia, Chem. Commun, Volume, 46, 5951-5953 (2010).
- [15] M. H. Maneshian, F. L. Kuo, K. Mahdak, J. Hwang, R. Banerjeeand N. D. Shepherd, Nanotechnology, Volume 22, 205703 (2011)
- [16] B. Seger and P. V. Kamat, J. Phys. Chem. C, Volume 113, 7990–7995 (2009)
- [17] H. Zhao, J. Yang, L. Wang, C. G. Tian, B. J. Jiang and H. G. Fu, Chem. Commun, Volume 47, 2014–2016 (2011).
- [18] R. Kumar, D. Varandani, B. R. Mehta, V. N. Singh, Z. H. Wen, X. L. Feng and K. Mullen, Nanotechnology, Volume 22, 275719 (2011).
- [19] T. V. Cuong, V. H. Pham, J. S. Chung, E. W. Shin, D. H. Yoo, S. H. Hahn, J. S. Huh, G. H.

## REFERENCES

- Rue, E. J. Kim, S. H. Hur and P. A. Kohl, *Mater. Lett.*, Volume 64, 2479–2482 (2010).
- [20] H. J. Song, L. C. Zhang, C. L. He, Y. Qu, Y. F. Tian and Y. Lv, *J. Mater. Chem.*, Volume 21, 5972–5977 (2011).
- [21] Z. X. Jiang, J. J. Wang, L. H. Meng, Y. D. Huang and L. Liu, *Chem. Commun.*, Volume 47, 6350–6352 (2011).
- [22] H. Y. Jeong, D. S. Lee, H. K. Choi, D. H. Lee, J. E. Kim, J. Y. Lee, W. J. Lee, S. O. Kim and S. Y. Choi, *Appl. Phys. Lett.*, 96, 213105 (2010).
- [23] John. Boardman, "The Neolithic-Eneolithic Period" *The Cambridge ancient history*, Volume 3, part1, 31-33.
- [24] P. R. Wallace, "The Band Theory of Graphite" *Physical Review* 1947, Volume 71, 476 (2010).
- [25] A. K. Geim, K. S. Novoselov, "The rise of graphene" *Nature Materials*, Volume 6, 183 (2007).
- [26] Re Peierls, "Quelques propriétés typiques des corps solides" *Ann. Inst. Henri Poincare*, Volume 5, 177 (1935)..
- [27] Ld Landau, "Zur theorie der phasenumwandlungen II. Phys" *Z. Sowjetunion* Volume 11, 26 (1937)..
- [28] Boehm, H. P.; Clauss, A.; Fischer, G. O.; Hofmann, U. *Zeitschrift FTIR anorganische und allgemeine Chemie (in German)* 316 (3–4): 119–127 (1962). [doi:10.1002/zaac.19623160303](https://doi.org/10.1002/zaac.19623160303).
- [29] B.C. Brodie, *Philosophical Transactions of the Royal Society of London*, 149, 249 (1859).
- [30] Gina Pischel, "Carbon carbon bonds: Hybridization" (2011)
- [31] Jean-Noël FUCHS, Mark Oliver GOERBIG, (2008).
- [32] L. Y. Jiao, L. Zhang, X. R. Wang, G. Diankov, H. J. Dai, *Nature*, Volume 458, 877 (2009).
- [33] X. T. Jia, M. Hofmann, V. Meunier, B. G. Sumpter, J. Campos-Delgado, J. M. Romo-Herrera, H. B. Son, Y. P. Hsieh, A. Reina, J. Kong, M. Terrones, M. S. Dresselhaus, *Science*, Volume 323, 1701 (2009).
- [34] Brian Shevitski "Structural Properties of Graphene and Carbon Nanotubes" CA 90095, (2010).
- [35] Farhan Rana "Carbon Nanotubes, physics and application" Handout Volume 31, (2009)
- [36] Prasanta K, Misra, chapter 18, "Physics of condensed Matter" University of Houston.

## REFERENCES

---

- [37] Luis E. F. Foa Torres, Stephan Roche, Jean-Christophe Charlier, published (2014).
- [38]. Pumera M., Chemical Society Review, Volume 39, 4146 (2010).
- [39] M. J. Allen, V. C. Tung, L. Gomez, Z. Xu, L. M. Chen, K. S. Nelson, C. W. Zhou, R. B. Kaner, Y. Yang, Advanced Materials, Volume 21, 2098 (2009).
- [40] Shirui Guo, Maziar Ghazinejad, Xiangdong Qin, Huaxing Sun, Wei Wang, Francisco Zaera, Cengiz S. Ozkan, Mihrimah Ozkan Small, Volume 8, 1073 (2012).
- [41] L. M. Dai, "Layered Graphene/Quantum Dots: Nanoassemblies for Highly Efficient Solar Cells" Chemsuschem, Volume 3, 797 (2010).
- [42] N. L. Yang, J. Zhai, D. Wang, Y. S. Chen, L. Jiang, Acs Nano, Volume 4, 887 (2010).
- [43] C. X. Guo, H. B. Yang, Z. M. Sheng, Z. S. Lu, Q. L. Song, C. M. Li, Angewandte Chemie-International Edition, Volume 49, 3014 (2010).
- [44] H. X. Chang, X. J. Lv, H. Zhang, J. H. Li, Electrochemistry Communications, Volume 12, 483 (2010).
- [45] Z. Y. Chen, S. Berciaud, C. Nuckolls, T. F. Heinz, L. E. Brus Acs, Nano, Volume 4, 2964 (2010)..
- [46] J. K. Wassei, R. B. Kaner, Materials Today, Volume 13, 52.38(2010)
- [47] V. C. Tung, L. M. Chen, M. J. Allen, J. K. Wassei, K. Nelson, R. B. Kaner, Y. Yang Nano Letters, Volume 9, 1949 (2009).
- [48] S. S. Li, K. H. Tu, C. C. Lin, C. W. Chen, M. Chhowalla, Acs Nano, Volume 4, 3169(2010).
- [49] G. Eda, M. Chhowalla, Advanced Materials, Volume 22, 2392(2010).
- [50] S. De, P. J. King, M. Lotya, A. O'Neill, E. M. Doherty, Y. Hernandez, G. S. Duesberg, J. N. Coleman, *Volume 58, 4 (2013)*.
- [51] Limei Zhu, Liqiang Luo, Zhenxin Wang, Biosensors and Bioelectronics, Volume 35, 507(2012).
- [52] F. Chen, J. L. Xia, N. J. Tao Nano Letters, Volume 9, 1621-1639(2009)
- [53] Y. Y. Shao, J. Wang, H. Wu, J. Liu, I. A. Aksay, Y. H. Lin Electroanalysis, Volume 22, 1027(2010).
- [54] Shi-Rui Guo, Jian Lin, Miroslav Penchev, Emre Yengel, Maziar Ghazinejad, Cengiz S. Ozkan, Mihrimah Ozkan, " J. Nanosci. Nanotechnol., Volume 11, 5258(2011).
- [55] Chen, X. M, Wu, G. H, & Jiang, Y. Q. Wang YRC, X. Graphene and graphene-based

## REFERENCES

- nanomaterials: The promising materials for bright future of electroanalytical chemistry. Analyst, Volume 136, 4631-40 (2011).
- [56] Graphene nanoplatelets, CAS 1034343-98, U.S, Registered trademark.(1998-2015).
- [57] Kamran ul Hassan” Graphene and ZnO Nanostructures for Nano- Optoelectronic & Biosensing Applications”(2012).
- [58] C. Jagadish and S. J. Pearton, “Zinc Oxide Bulk, Thin Films and Nanostructures Processing, Properties and Application” Elsevier (2006).
- [59] Z. L. Wang, J.Phys.,Condens. Matter, Volume 16,829–858(2004)
- [60] Z.L. Wang, J. Phys. Condensed Matter, Volume, 16 , 829 (2004).
- [61] G.H. Lee, Y. Yamamoto , M. Kourogia, M. Ohtsua, Thin Solid Films, Volume 386. 117 -120,(2001).
- [62] M. Risti et al.,Journal of Alloys and Compounds ,Volume 397, L1–L4(2005).
- [63] K. H. Hellwege, O. Madelung, A. M. Hellege, Volume 19,119-595 (1987).
- [64] E. D. Eastman,J. Am. Chem. Soc., 1924, 46 (4), pp 917–923,DOI: 10.1021/ja01669a014, Publication Date: April (1924).
- [65] JAMES PAWLEY” The Development of Field-Emission Scanning Electron Microscopy for Imaging Biological Surfaces” SCANNING Volume. 19, 324-336 (1997).
- [66] McHenry, M., Soffa, W.A., Preface to viewpoint set on: L10 phases for permanent magnet and recording applications, Scripta Materialia, Volume 53, p. 381-382( 2005).
- [67] Thermo nicolet corporation”Introduction to Fourier Transform Infrared spectrometry”(2001)
- [68] G. D. Gilliland, Mater. Sci. Eng.,Volume 99, R18 (1997).
- [69] Halvorson, R. A.; Vikesland, P. J., Volume 44 (20), 7749-7755(2010).
- [70] L Djellala, A Bougueliab, H M Kadi, M Trarib, Sol. Ener. Mater. Solar Cells Volume 92 , 594 (2008).
- [71] Spliethoff JW, Evers DJ, Klomp HM, van Sandick JW, Wouters MW, Nachabe R, Lucassen GW, Hendriks BHW, Wesseling J, Ruers TJM,, Lung Cancer,Volume 80, pp 165– 171 (2013).
- [72] S.Gayathr,P.Jayabal,M.Kattaisamy and V. Ramakrishnan,Journal of Applied Physics Volume 115,173504 (2014)

## REFERENCES

---

- [73] Park, C. H., J. S. Lopez, and C. B. Cook, Volume 13: 318-320 (1978).
- [74] A. C. Ferrari, Solid State Commun. Volume 143, 47-57 (2007).
- [75] M. J. Allen, V. C. Tung, L. Gomez, Z. Xu, L. M. Chen, K. S. Nelson, C. W. Zhou, R. B. Kaner, Y. Yang, Advanced Materials, Volume 21, 2098(2009).
- [76] Shirui Guo, Maziar Ghazinejad, Xiangdong Qin, Huaxing Sun, Wei Wang, Francisco Zaera, Cengiz S. Ozkan, Mihrimah Ozkan Small, Volume 8, 1073(2012).
- [77] L. M. Dai, Chemsuschem, Volume 3, 797 (2010).
- [78] N. L. Yang, J. Zhai, D. Wang, Y. S. Chen, L. Jiang, Acs Nano, Volume 4, 887 (2010).
- [79] C. X. Guo, H. B. Yang, Z. M. Sheng, Z. S. Lu, Q. L. Song, C. M. Li, Angewandte Chemie-International Edition, Volume 49, 3014 (2010).
- [80] H. X. Chang, X. J. Lv, H. Zhang, J. H. Li, Electrochemistry Communications, Volume 12, 483(2010).
- [81] Z. Y. Chen, S. Berciaud, C. Nuckolls, T. F. Heinz, L. E. Brus ACS Nano, Volume 4, 2964(2010).
- [82] J. K. Wassei, R. B. Kaner, Materials Today, Volume 13, 52.38 (2010).
- [83] N.Y. Garces, L.Wang, L.Bai, N.C.Giles, L.E.Halliburton, G.Cantwell, Applied Physics Letters 81, 622-624 (2002).
- [84] S. S. Li, K. H. Tu, C. C. Lin, C. W. Chen, M. Chhowalla, Acs Nano, Volume 4, 3169(2010).
- [85] G. Eda, M. Chhowalla, Advanced Materials, Volume 22, 2392(2010).
- [86] S. De, P. J. King, M. Lotya, A. O'Neill, E. M. Doherty, Y. Hernandez, G. S. Volume 58, 4 (2013)
- [87] Kang S, Herzberg M, Rodrigues DF, Elimelech M. Langmuir; Volume 24:6409-13(2008).
- [88] Espitia PJP, Soares NFF, Coimbra JSR, Andrade NJ, Cruz RS, Medeiros EAA. Food Bioprocess Technol. Volume 5:1447-1464(2012).
- [89] B.Cao, S.Cao, P. Dong, J. Gao, J. Wang, Mater.Lett. Volume 93, 349-352 (2013).
- [90] Li, Y., Leiyong, Li., Chenwan, Li., Chen, W., & Zeng, M. Applied Catalysis A: General, 427(428), 1-7(2012).

*Dr. Javed Iqbal Saggu*  
Assistant Professor (Physics)  
International Islamic University  
Islamabad

## 7 Plagiarism Report

Final November, 2015 MS Thesis

Synthesis and Characterization of ZnO based Graphene Nanoplatelets Nanocomposites by Muhammad Saleem

From BS, MS and PhD Thesis (BS, MS, Ph.D Thesis Plagiarism)

Processed on 03-Nov-2015 12:32 PKT

**ID: 594409043**

Word Count: 10974

**Similarity Index: 7%**

Similarity by Source

Internet Sources: 2%

Publications: 4%

Student Papers: 3%

**Sources:**

1. 1% match (student papers from 30-Aug-2012)

Submitted to Higher Education Commission Pakistan on 2012-08-30

2. < 1% match (publications)

Bai. Song, and Xiaoping Shen. "Graphene inorganic nanocomposites". RSC Advances, 2012.

3. < 1% match (student papers from 16-Mar-2013)

Submitted to Institute of Graduate Studies, UiTM on 2013-03-16

4. < 1% match (student papers from 03-Jan-2012)

Submitted to University of Leeds on 2012-01-03

5. < 1% match (Internet from 01-Mar-2015)

<http://ecl.uovs.ac.za/ETD-db/theses/available/etd-08042014-122410/unrestricted>

TshabalalaMA.pdf

6. < 1% match (publications)

Springer Series in Materials Science, 2014.

7. < 1% match (student papers from 20-Mar-2015)

Submitted to Higher Education Commission Pakistan on 2015-03-20

8. < 1% match (Internet from 22-Mar-2014)

[http://www.chem.uconn.edu/~hsz/edu5776/photometry\\_manuals/OU.edu\\_CCD\\_photometry\\_wreed06.pdf](http://www.chem.uconn.edu/~hsz/edu5776/photometry_manuals/OU.edu_CCD_photometry_wreed06.pdf)

9. < 1% match (student papers from 28-Aug-2012)

10. < 1% match (publications)

Yan, Abdullah. "Electron-vibron effects in interacting quantum dot systems", Publikationsserver der Universität Regensburg, 2012.

11. < 1% match (student papers from 17-Jul-2014)

Submitted to Indian Institute of Technology, Kharagpure on 2014-07-17

12. < 1% match (student papers from 29-Jun-2015)

Submitted to International Islamic University Malaysia on 2015-06-29

13. < 1% match (publications)

Gusatti, Marivone, Carlos Eduardo Maduro De Campos, Gilvan SÃ©rgio Barroso, Daniel AragÃ£o Ribeiro De Souza, Humberto Gracher Riella, and Nivaldo Cabral Kuhnen. "Preparation and Characterization of ZnO Nanostructures with Different Precursors via Solochemical Technique", Applied Mechanics and Materials, 2011.

14. < 1% match (publications)

Li, Guofang, Yahui Xia, Yanbao Zhao, Ping Li, Fuqiang Zhang, and Peng Qu. "Solid?Liquid Reaction Synthesis of High-Purity Potassium Hexathionate and Its Antibacterial Properties",

Australian Journal of Chemistry, 2015.

15. < 1% match (publications)

Siddique. Yasir Hasan Khan, Wasi Khanam,. "Toxic potential of synthesized graphene zinc oxide nanocomposite in the third instar larvae of trans", BioMed Research International, Annual 2014

16. < 1% match (publications)

Wang. Hou, Xingzhong Yuan, Yan Wu, Huajun Huang, Xin Peng, Guangming Zeng, Hua Zhong, Jie Liang, and MiaoMiao Ren. "Graphene-based materials: Fabrication, characterization and application for the decontamination of wastewater and wastegas and hydrogen storage/generation", Advances in Colloid and Interface Science, 2013.

17. < 1% match (Internet from 30-Jun-2015)

<http://www.jnanobiotechnology.com/content/pdf/1477-3155-11-39.pdf>

18. < 1% match (publications)

MAHITO KOHMOTO. "GAUGE FIELDS, QUANTIZED FLUXES AND MONOPOLE CONFINEMENT OF THE HONEYCOMB LATTICE", International Journal of Modern Physics B, 2009

19. < 1% match (student papers from 19-Dec-2014)

Submitted to Universiti Teknologi MARA on 2014-12-19

20. < 1% match (Internet from 09-Feb-2014)

<http://bi.tbzmed.ac.ir/Portals/0/BI-2013/Baker-BioImpacts-2013.pdf>

21. < 1% match (publications)

Lin, X.. "Enhanced photocatalytic activity of fluorine doped TiO<sub>2</sub> by loaded with Ag for degradation of organic pollutants", Powder Technology, 201203

22. < 1% match (student papers from 24-Apr-2014)

Submitted to University of Southampton on 2014-04-24

23. < 1% match (student papers from 02-Jun-2014)

Submitted to Universiti Teknologi MARA on 2014-06-02

24. < 1% match (Internet from 27-Sep-2014)

<http://herkules.oulu.fi/isbn9789526205489/isbn9789526205489.pdf>

25. < 1% match (Internet from 20-May-2015)

[http://www.hgky.net/en/nd.jsp?id=124&\\_np=2\\_349](http://www.hgky.net/en/nd.jsp?id=124&_np=2_349)

26. < 1% match (publications)

Essabir, Hamid, Mounir El Achaby, El Moukhtar Hilali, Rachid Bouhfid, and AbouElkacem Qaiss. "Morphological, Structural, Thermal and Tensile Properties of High Density Polyethylene Composites Reinforced with Treated Argan Nut Shell Particles", Journal of Bionic Engineering, 2015.

27. < 1% match (student papers from 25-Apr-2015)

Submitted to Iona College on 2015-04-25

28. < 1% match (student papers from 16-Mar-2015)

Submitted to Shivaji University on 2015-03-16

29. < 1% match (student papers from 04-Sep-2012)

<https://www.researchgate.net/publication/26112409001>

30. < 1% match (student papers from 19-Apr-2015)

Submitted to University of Babylon on 2015-04-19

31. < 1% match (student papers from 19-May-2010)

Submitted to Asian Institute of Technology on 2010-05-19

32. < 1% match (Internet from 16-Apr-2010)

<http://ethesis.helsinki.fi/julkaisut/mat/kemia/vk/jernstrom/developm.pdf>

33. < 1% match ()

<http://www.drugholding.org/Page479.htm>

34. < 1% match (Internet from 16-Jun-2009)

<http://www.qub.ac.uk/qc/webpages/whatwedo/researchgroups/environmentalmodelling/ia/documents/chapter4.pdf>

35. < 1% match (publications)

Zhao, X.Q.. "Effects of thermal annealing temperature and duration on hydrothermally grown ZnO nanorod arrays", Applied Surface Science, 20090315

36. < 1% match (publications)

Nogueira, I. C., L. S. Cavalcante, P. F. S. Pereira, M. M. de Jesus, J. M. Rivas Mercury, N. C. Batista, M. Siu Li. and E. Longo. "Rietveld refinement, morphology and optical properties of  $(\text{Ba}_{1-x}\text{Sr}_x)\text{MoO}_4$  crystals", Journal of Applied Crystallography, 2013.

37. < 1% match (student papers from 01-Mar-2012)

Submitted to University of Strathclyde on 2012-03-01

38. < 1% match (Internet from 13-Feb-2014)

<http://www.mrs.org/spring-2014-call-for-papers-d/>

39. < 1% match (Internet from 17-Apr-2015)

<http://www.science.gov/topicpages/t/temperature+annealing+effects.html>

40. < 1% match (Internet from 14-Sep-2014)

[http://run.unl.pt/bitstream/10362/5380/1/Barquinha\\_2010.pdf](http://run.unl.pt/bitstream/10362/5380/1/Barquinha_2010.pdf)

41. < 1% match (Internet from 19-Mar-2014)

<http://www.doestoc.com/docs/12356546/Semiconductor-Characterization>

42. < 1% match (publications)

Sarawuth Labuayai. "Synthesis and optical properties of nanocrystalline ZnO powders prepared by a direct thermal decomposition route", Applied Physics A, 03/2009

---

43. < 1% match (publications)

Abbasi, Mazhar Ali, Yaqoob Khan, Sajjad Hussain, Omer Nur, and Magnus Willander. "Anion effect on the low temperature growth of ZnO nanostructures", Vacuum, 2012.

44. < 1% match (publications)

Shamsudin, M.S., and S.M. Sanip. "A Review on Graphene Evidenced by Raman Spectroscopy", Advanced Materials Research. 2015.

45. < 1% match (publications)

Viktor M. Kryachek. "Friction Composites: Traditions and New Solutions (Review). Part 2. Composite Materials", Powder Metallurgy and Metal Ceramics, 01/2005

46. < 1% match (publications)

Maity, Jyoti Prakash, Tz-Jiun Lin, Henry Pai-Heng Cheng, Chien-Yen Chen, A. Satyanarayana Reddy, Shashi B. Atla, Young-Fo Chang, Hau-Ren Chen, and Chien-Cheng Chen. "Synthesis of Brushite Particles in Reverse Microemulsions of the Biosurfactant Surfactin", International Journal of Molecular Sciences, 2011.

47. < 1% match (publications)

Momose, Atsushi, Wataru Yashiro, Masafumi Moritake, Yoshihiro Takeda, Kentaro Uesugi, Akihisa Takeuchi, Yoshio Suzuki, Makoto Tanaka, and Tadashi Hattori. "", Developments in X-Ray Tomography V. 2006.